Published in final edited form as:

Sci Transl Med. 2016 April 27; 8(336): 336ra62. doi:10.1126/scitranslmed.aaf0618.

Initiation of immune tolerance–controlled HIV gp41 neutralizing B cell lineages

Ruijun Zhang[1,*], **Laurent Verkoczy**[1,2,3,*], **Kevin Wiehe**[1,3,*], **S. Munir Alam**[1,2,3,*], **Nathan I. Nicely**[1], **Sampa Santra**[4], **Todd Bradley**[1,3], **Charles W. Pemble IV**[1], **Jinsong Zhang**[1], **Feng**

‡Corresponding authors. barton.haynes@duke.edu (B.F.H.); l.liao@dm.duke.edu (H.-X.L.).
*These authors contributed equally to this work.
†Present address: BioMarin Pharmaceutical Inc., 105 Digital Drive, Novato, CA 94949, USA.

SUPPLEMENTARY MATERIALS

www.sciencetranslationalmedicine.org/cgi/content/full/8/336/336ra62/DC1

Fig. S1. Rhesus macaque immunization regimen, reactivity of serum and mucosal fluids, and neutralization of HIV isolates.
Fig. S2. B cell repertoires of macaques 584 and 585.
Fig. S3. Rhesus macaque clonal lineages using V_H and V_L genes similar to 2F5V_H/V_L.
Fig. S4. Neutralization by members of the DH570 clone.
Fig. S5. Amino acid and lipid insertion propensity differences within the three DH570 lineage members for which crystal structures were determined.
Fig. S6. Binding of DH570 lineage antibodies to MPER liposomes.
Fig. S7. Replicate images for Fig. 1A.
Fig. S8. Replicate images for Fig. 1E.
Fig. S9. Replicate plots for Fig. 5.
Fig. S10. Representative mouse flow cytometry gating strategies.
Fig. S11. Representative rhesus flow cytometry gating strategies.
Table S1. Neutralization of HIV isolates by DH573.
Table S2. Neutralization of HIV isolates by the DH570 clonal lineage.
Table S3. Characteristics of the DH570 clonal lineage isolated from rhesus macaque 585.
Table S4. Time course for HIV neutralization in the TZM-bl/FcgRI assay.
Table S5. Data collection and refinement statistics.
Table S6. Kinetic rates of DH570 lineage members from branch I and IV binding to MPER peptide-liposomes by BLI.
Table S7. CDR3 lipid insertion propensity for select DH570 lineage members.
Table S8. Statistical analysis summary for Fig. 1.

Author contributions: R.Z. performed isolation and expression of antibodies and wrote and edited the paper; L.V. constructed and studied the knock-in mice and edited the paper; K.W. performed antibody analyses, oversaw the computational analysis of antibody sequences, designed antibody mutants, and wrote and edited the paper; S.M.A. performed SPR and BLI and wrote and edited the paper; N.I.N. and C.W.P. performed crystallization analyses and wrote and edited the paper; S.S. led the macaque immunization studies; T.B. performed genomic analysis of antibodies and made antibody mutants; J.Z. performed studies on knock-in mice; F.G. performed sequencing of antibodies; D.C.M. performed neutralization assays; H.B.-V. performed immunizations of knock-in mice; G.K. performed autoreactivity assays and edited the paper; K. Larimore and P.D.G. provided the UA 2F5 knock-in $V_\kappa J_\kappa$ gene; R.P. performed antibody reactivity assays; A.F. expressed antibodies in transient transfections; J.N.P. performed mucosal antibody assays; K. Luo and X.L. isolated and expressed antibodies; A.M.T. analyzed antibody sequences; N.V. performed statistical analysis; G.D.T. performed antibody-binding assays; T.B.K. analyzed antibody sequences; M.A.M. oversaw antibody isolation and labeled memory B cell peptide hook reagents; H.-X.L. oversaw peptide synthesis, antibody isolation, and expression; B.F.H. conceived and designed the experiments, oversaw the study, evaluated all data, and wrote and edited the paper.

Competing interests: The authors declare competing financial interests: B.F.H., S.M.A., and H.-X.L. have patent applications submitted on vaccine candidates used in this study (see international patent application PCT/US06/13684 entitled, “Method of inducing neutralizing antibodies to human immunodeficiency virus.”

Accession codes: Coordinates and structure factors have been deposited in the Protein Data Bank under accession codes 5DD1 (DH570), 5DD3 (DH570.4), 5DD5 (DH570.9), and 5DD0 (DH570/MPER peptide complex). Gene sequences of the reported antibodies have been deposited in Genbank with the accession codes KX099066 - KX099167.

Ethics statement: This study using rhesus macaques was carried out in strict accordance with the recommendations in the *Guide for the Care and Use of Laboratory Animals* of the NIH at BIOQUAL Inc. BIOQUAL is fully accredited by Association for Assessment and Accreditation of Laboratory Animal Care and through Office of Laboratory Animal Welfare assurance no. A-3086. The protocol was approved by the BIOQUAL IACUC. All physical procedures associated with this work were done under anesthesia to minimize pain and distress.

Gao[1,3], **David C. Montefiori**[1,5], **Hilary Bouton-Verville**[1], **Garnett Kelsoe**[1,6], **Kevin Larimore**[7,†], **Phillip D. Greenberg**[7], **Robert Parks**[1], **Andrew Foulger**[1], **Jessica N. Peel**[1], **Kan Luo**[1], **Xiaozhi Lu**[1], **Ashley M. Trama**[1], **Nathan Vandergrift**[1,3], **Georgia D. Tomaras**[1,5], **Thomas B. Kepler**[8], **M. Anthony Moody**[1,6,9], **Hua-Xin Liao**[1,3,‡], and **Barton F. Haynes**[1,2,3,‡]

[1]Duke Human Vaccine Institute, Duke University School of Medicine, Durham, NC 27710, USA.

[2]Department of Pathology, Duke University School of Medicine, Durham, NC 27710, USA.

[3]Department of Medicine, Duke University School of Medicine, Durham, NC 27710, USA.

[4]Beth Israel Deaconess Medical Center, Boston, MA 02215, USA.

[5]Department of Surgery, Duke University School of Medicine, Durham, NC 27710, USA.

[6]Department of Immunology, Duke University School of Medicine, Durham, NC 27710, USA.

[7]Fred Hutchinson Cancer Research Center, University of Washington, Seattle, WA 98109, USA.

[8]Department of Microbiology, Boston University School of Medicine, Boston, MA 02118, USA.

[9]Department of Pediatrics, Duke University School of Medicine, Durham, NC 27710, USA.

Abstract

Development of an HIV vaccine is a global priority. A major roadblock to a vaccine is an inability to induce protective broadly neutralizing antibodies (bnAbs). HIV gp41 bnAbs have characteristics that predispose them to be controlled by tolerance. We used gp41 2F5 bnAb germline knock-in mice and macaques vaccinated with immunogens reactive with germline precursors to activate neutralizing antibodies. In germline knock-in mice, bnAb precursors were deleted, with remaining anergic B cells capable of being activated by germline-binding immunogens to make gp41-reactive immunoglobulin M (IgM). Immunized macaques made B cell clonal lineages targeted to the 2F5 bnAb epitope, but 2F5-like antibodies were either deleted or did not attain sufficient affinity for gp41-lipid complexes to achieve the neutralization potency of 2F5. Structural analysis of members of a vaccine-induced antibody lineage revealed that heavy chain complementarity-determining region 3 (HCDR3) hydrophobicity was important for neutralization. Thus, gp41 bnAbs are controlled by immune tolerance, requiring vaccination strategies to transiently circumvent tolerance controls.

INTRODUCTION

Induction of broadly reactive neutralizing antibodies (bnAbs) is a critical priority for HIV vaccine development. However, no vaccine regimen has been able to induce bnAbs to conserved HIV envelope (Env) epitopes (1, 2). Previous work has used stabilized HIV Env trimers or engineered Env epitopes to prime bnAb lineages in knock-in mice (3, 4), but stabilized native-like trimers have induced only autologous neutralizing antibodies (5) and induced dominant nonneutralizing antibody specificities (6) similar to nonnative Env trimers (7). Explanations for the inability to elicit bnAbs include the lack of fully native trimer immunogens (2), inability of immunogens to bind to the un-mutated (germline) ancestors (UAs) of bnAbs (8), and inability to mimic the precise series of sequential immunogens that drive bnAb production in natural infection (9).

Env-targeted bnAbs 2F5, 4E10, and 10E8 bind to the membrane-proximal external region (MPER) of gp41 and are autoreactive (10–12). These bnAbs use hydrophobic heavy chain complementarity-determining region 3 (HCDR3) to bind to virions in a two-step model, tethering them to the virion lipid membrane, thus enabling them to be present before CD4-induced exposure of their epitopes on the gp41 hairpin intermediate Env conformation (13–15). Whereas the first binding step is a relatively unspecific interaction with the viral lipid membrane (13, 14, 16), the second binding step is the stable docking of the bnAb to gp41 MPER motifs composed of both lipids and gp41 MPER (13, 14, 16–19). When matured (that is, mutated and selected for high affinity) 2F5 and 4E10 bnAb V_HDJ_H/V_LJ_L genes are expressed in knock-in mice, B cell development is limited by immune tolerance deletion and anergy (20–23), but the question of whether the germline UA antibodies of MPER bnAbs are also controlled by tolerance remains unanswered. To answer this question, we designed immunogens (17, 19, 24) that avidly bind the UA of the 2F5 bnAb to immunize 2F5 knock-in mice and rhesus macaques to determine their ability to initiate and drive gp41 bnAb lineages to maturation.

RESULTS

Vaccination of 2F5 germline mice

We constructed a 2F5 germline/UA double knock-in (dKI; $V_HDJ_H^{+/+}$ + $V_\kappa J_\kappa^{+/+}$) mouse to determine whether the 2F5 germline UA is controlled by immune tolerance and, if so, whether any remaining B cells can be activated to clonally expand. About 98% of 2F5 UA B cell receptor (BCR)–bearing B cells were deleted at the immature/transitional B cell stage in bone marrow (Fig. 1A) and ~1 to 2% residual B cells entered peripheral tissues (Fig. 1B), predominantly accumulating as transitional B cells (Fig. 1C) with down-modulated BCR densities (Fig. 1D) and mitigated calcium signaling in response to BCR crosslinking (Fig. 1E), features consistent with anergy (20, 25). We next immunized 2F5 germline/UA dKI mice with gp41 peptide-liposomes known to mimic virion interactions with 2F5 and 4E10 MPER bnAbs (13, 19) and to have a strong affinity for the 2F5 UA (26). We found that residual germline 2F5 UA KI^+ splenic newly formed/transitional B cells with gp41 2F5 epitope reactivity could be activated by immunization to clonally expand and increase BCR density (Fig. 1F), but most had not isotype-switched (Fig. 1G). Similarly, serum antibody activity for gp41 2F5 epitope peptides was predominantly immunoglobulin M (IgM) (Fig. 1H). Thus, in 2F5 UA KI mice, 2F5 UA–expressing B cells were controlled by central tolerance, and despite their activation and expansion by immunization with gp41 peptide-liposomes, their further expansion and/or differentiation into the mature B cell compartment were limited.

Vaccination of rhesus macaques

To determine whether 2F5-like antibody lineages could be initiated in primates, we immunized rhesus macaques with a set of Env immunogens designed to bind 2F5 and 4E10 germline UAs (14, 15, 24, 26), by priming with recombinant vaccinia virus (rVV)–expressing JRFL gp140, boosting twice with deglycosylated JRFL gp140, followed by repetitive boosting with gp41 peptide-liposomes mixed with Toll-like receptor 4 (TLR4), TLR7/8, and TLR9 agonists (fig. S1A). After gp140/MPER peptide-liposome

immunizations, antibodies to HIV Env gp140 (fig. S1B) and MPER 2F5 epitope peptide (fig. S1C) were induced in all four macaques. In two macaques (R584 and R585), the immunization regimen appeared to break tolerance, eliciting plasma antibodies that bound kynureninase, a host protein that contains the 2F5 epitope amino acids 662 to 667 (ELDKWA) (fig. S1D), but did not bind to a mutant kynureninase (ELEKWA) that abrogates 2F5 binding (11) nor bound to the 4E10 bnAb epitope (fig. S1, E and F). Plasma antibodies only neutralized easy-to-neutralize (tier-1) viruses in the TZM-bl assay (fig. S1G). In addition to plasma, antibodies to the MPER were detectable in rectal fluids after MPER peptide-liposome boosting (fig. S1H).

Characteristics of the 2F5 bnAb determined to be important for virion binding and neutralization are a long, hydrophobic HCDR3 (18) containing prolines (27) and a leucine-phenylalanine residue pair (13) critical for lipid reactivity. In HCDR2, an aspartic acid triplet (DDD) and a pair of arginines at the base of HCDR3 contribute to interactions with complementary charged amino acids in the MPER (28, 29). To search for vaccine-induced antibodies with these characteristics that used a V_H gene similar to the 2F5 (V_H2–5), we performed next-generation sequencing (NGS). We detected V_HDJ_H sequences at 16 and 24 weeks after rVV-JRFL gp140 immunization with the above 2F5-like characteristics but did not detect similar sequences at either week 92 or week 150 after immunization (fig. S2, A and B). Thus, antibodies most similar to 2F5 fell to below the threshold of detection by NGS after the week 24 immunization, suggesting B cell deletion.

Next, MPER-specific memory B cells were sorted by flow cytometry from peripheral blood mononuclear cells (PBMCs) of macaques R584 and R585 using a fluorophore-labeled gp41 heptad repeat-2 (HR-2) tetrameric peptide (MPER.03), previously shown to bind to MPER bnAb memory B cells (fig. S2C) (30). We isolated a total of 549 antibodies that either were gp41 MPER-reactive or used the rhesus genes similar to those of 2F5 V_H (variable region of Ig heavy chain) and V_L (variable region of Ig light chain) (fig. S2, D and E). We identified 33 B cell clonal lineages, 3 of which used rhesus V_H2 and $V_κ1$ genes that are similar to the HIV bnAb 2F5 V_H2–5, V_k1–13 genes (clones DH571 and DH572 from macaque R585, and clone DH573 from macaque R584) (fig. S3, A to F). Clones DH571 and DH572 did not react with gp41 MPER, whereas DH573 reacted with gp41 MPER and kynureninase but not with mutant kynureninase, indicating specificity for the ELDKWA neutralizing epitope (fig. S3F) (11).

To assess neutralization by MPER antibodies, we used the TZM-bl assay and the TZM-bl/FcγRI assay that uses TZM-bl epithelial cells transfected with CD64 (FcγRI), thus enabling the cells to bind MPER bnAbs and augment their ability to associate with the virion before receptor-mediated activation. This assay is highly sensitive for MPER antibodies by using a cell line that provides a kinetic advantage for the antibody to access the transiently exposed MPER epitope (fig. S4B) (31, 32). The MPER-reactive antibody DH573 could not neutralize HIV in either assay (table S1) because of limited monoclonal antibody (mAb) recognition of gp41 peptidelipid complexes (fig. S3, F and G). Thus, antibodies with 2F5-like V_H/V_L pairings were induced by vaccination, but these antibodies did not react with MPER pep-tide in the context of liposomes nor neutralize HIV.

Induced macaque neutralizing antibodies

We next performed neutralization assays on 94 representative antibodies that either shared 2F5 V_H and V_L characteristics or bound the gp41 MPER, and found one antibody, DH570, that neutralized both tier 1 and tier 2 heterologous HIV strains in the TZM-bl/FcγRI assay but not in the TZM-bl assay (Fig. 2). We isolated 77 natural antibody V_HDJ_H and V_LJ_L gene pairs within clone DH570 from weeks 43 to 144 of immunization and produced 32 for study (Fig. 2A and tables S2 and S3). Analysis of the DH570 clone revealed five branches in the lineage and use of a 2F5-like light chain (rhesus V_k1–23) paired with a V_H4 heavy chain (Fig. 2, A and B, and table S3). We assayed antibody clonal lineage members including the inferred unmutated common ancestor (UCA), intermediate antibodies (IAs) and natural V_H and V_L paired antibodies for binding to HIV Env gp140, gp41, GCN4-gp41-inter [a construct reflective of the gp41 intermediate conformation epitope neutralized by gp41 bnAbs (33)], and the 2F5 nominal epitope peptide (table S3), as well as for polyreactivity (table S3). We noted increasing affinity for gp41 epitopes during the maturation of the DH570 lineage and sporadic appearance of polyreactivity to cellular antigens (table S3). Only lineage branches I and IV contained multiple members that neutralized HIV in the TZM-bl/FcγRI assay (Fig. 2, A and C, and table S2). Neutralization capacity of DH570 members was in general weak and did not reach 100% neutralization of isolates tested in the TZM-bl/FcγRI assay (fig. S4A).

The neutralization epitope for gp41 bnAbs is transiently exposed after CD4 binding to Env, resulting in a window of time during which bnAbs can bind the MPER (31, 32, 34). We determined the window of time [half-life ($t_{1/2}$) of neutralization] during which clone DH570 antibodies could neutralize various strains of HIV (32, 34, 35). We found that although bnAb 2F5 was able to neutralize the tier 1 clade B HIV isolate W61D in the TZM-bl/FcγRI assay with $t_{1/2}$ = 68.8 ± 20.7 min, and the tier 2 clade B HIV isolate SC422661 with $t_{1/2}$ = 31.0 ± 5.6 min, DH570 lineage members had an estimated $t_{1/2} \leq 10$ min against HIV W61D or SC422661 in the TZM-bl/FcγRI assay (table S4). These data demonstrated that DH570 lineage antibodies have a limited window of time to access the transiently exposed MPER epitope that can only be partially compensated by their interaction with FcγRI on TZM-bl cells (fig. S4B). To estimate the relevance of DH570 antibodies to in vivo HIV infection, we reasoned that if the determining feature of the TZM-bl/FcγRI assay was target cell surface expression of FcγRI, then the DH570 lineage should potently neutralize tier 2 HIV strains in $CD4^+$, $Fc\gamma RI^+$ monocyte/macrophages (36). Vaccine-induced mAb DH570 mediated neutralization of the clade B tier 2 HIV strain JRFL in cultured monocyte/macrophages with an IC_{80} (80% inhibitory concentration) of 0.61 μg/ml (fig. S4, C and D).

Structures of DH570 lineage antibodies

We solved the cocrystal structure of antibody DH570 bound to the gp41 MPER nominal epitopecontaining peptide ($gp41_{660–670}$) at 2.5 Å resolution (Fig. 3, A and B, and table S5). The gp41 MPER peptide adopted a helical conformation in proximity to the HCDR3 (Fig. 3, A and B). Residues in HCDR3, including an apical phenylalanine (Phe^{100D}), formed a hydrophobic cleft that accommodated MPER Trp^{666} (Fig. 3B). DH570 HCDR2 residues Arg^{56} and Glu^{58} formed salt-bridge interactions with Glu^{664} and Lys^{665} of the gp41 epitope, respectively (the same MPER residues with which 2F5 forms salt-bridge interactions) (Fig.

3B). Unlike 2F5, the DH570 light chain did not interact with the gp41 peptide (Fig. 3B). Both DH570 and 2F5 adopted similar HCDR3 structures having an extended conformation with hydrophobic residues at the apices available for lipid-membrane interactions, but the HCDR3s exhibited different approach angles relative to their MPER epitopes (Fig. 3B).

To determine any structural basis for differing neutralization capacities, crystal structures of three unliganded DH570 antibody Fab fragments, including neutralizing antibodies DH570 and DH570.4 and nonneutralizing antibody DH570.9, were resolved to 1.6, 1.8, and 1.9 Å, respectively (Fig. 3A and table S5). The overall structures of the three antibodies were similar and exhibited similar HCDR3 conformations owing to identical HCDR3 sequences, suggesting that differences in their neutralization capacities were due to differences in the biochemical character of their paratopes outside of the HCDR3 (fig. S5). Lipid insertion propensity, a designation of amino acid hydrophobicity (37) shown to be highly correlated with 2F5 neutralization (38), was much higher in the LCDR3 of neutralizing members DH570 and DH570.4 than the nonneutralizing DH570.9 (fig. S5, B and C). Overall, lipid insertion propensity of the HCDR3 and LCDR3 was significantly more favorable for neutralizing members of the DH570 clonal lineage than nonneutralizing members (Fig. 4A). Thus, it is likely that antibody capacity to interact with lipid is as essential for neutralization potency for the DH570 clone as it is for the 2F5 bnAb.

Kinetic rate map of DH570 binding

We reasoned that if tolerance mechanisms exerted evolutionary constraints on affinity maturation of the DH570 antibody lineage, then the DH570 lineage would mature toward the affinity of 2F5, but a ceiling of affinity maturation would be observed below that of the 2F5 bnAb. Because the MPER epitope is exposed transiently during the postreceptor-triggered state of Env (33, 34), faster association rates during the initial encounter with antigen and formation of stable complexes with slower dissociation rates are critical kinetic parameters that allow the antibodies to engage the MPER epitope associated with lipids as is present on HIV virions (13, 14). We have previously shown that MPER bnAbs bind to both HIV virions and to MPER peptide-liposomes in a two-step manner, and that MPER peptide-liposome binding of gp41 bnAbs mirrors bnAb binding to virions (13, 14). Thus, using MPER peptide-liposomes, we found that although the dissociation rates of the DH570 branch I and IV antibodies approached that of 2F5, the association rates were an order of magnitude slower (range, 5- to 31-fold slower) (Fig. 4, B to D).

In branch IV, affinity maturation from IA76 to IA47 achieved dissociation and association rates closest to bnAb 2F5, with IA47 achieving the best neutralization of HIV in the TZM-bl/FcγRI but not the TZM-bl assay (table S2), indicating that the 2F5 antibody association rate of $5 \times 10^5\ M^{-1}\ s^{-1}$, a rate that approaches simple diffusion processes (39), may be required for HIV bnAb activity in the absence of tethering to the viral membrane. Along with having the fastest association rate, IA47 also had the most favorable HCDR3 lipid insertion propensity score of the DH570 clonal lineage (table S7) and overall HCDR3 lipid insertion propensity score was correlated with association rate (Spearman's rank correlation $\rho = -0.53$; tables S6 and S7). Of the six descendants of IA47, antibodies DH570.16, DH570.17, and DH570.19 accumulated V_H mutations (to 14%) that moderately reduced

their HCDR3 lipid insertion propensity (table S7). Whereas their dissociation rates improved, their association rates declined (four- to fivefold), and concomitantly, neutralization breadth for these antibodies decreased compared to IA47 (table S2), further underscoring the critical role association rate plays in the mechanism of neutralization in the DH570 lineage. HCDR3 lipid insertion propensity of the remaining three descendants of IA47 decreased even further, and two antibodies, DH570.20 and DH570.21, accrued V_H mutations up to ~21%, which resulted in their complete loss of neutralization in the TZM-bl/FcγRI assay due to profound declines in their association and dissociation rates. Remarkably, DH570.20 and DH570.21 reverted back to the kinetic rates of the DH570 UCA for MPER liposome binding (Fig. 4D) while maintaining binding to protein (table S3). Thus, these data are consistent with lowering of a ceiling for association rates of the MPER peptide-liposome–induced DH570 lineage such that bnAb potency could not be achieved (Fig. 4, B and C).

Mutations that improve neutralization

Finally, we asked whether introducing mutations derived from the HCDR3 of a DH570 lineage antibody (IA47) could increase the association rate and thus correct the TZM-bl assay neutralization deficit in the DH570 antibody. We hypothesized that combining the fast association rate of DH570.IA47 with the slower dissociation rate of DH570 could maximize MPER peptide-liposome binding and allow for neutralization in the TZM-bl neutralization assay in the absence of FcγRI. We introduced two amino acid substitutions (Asn^{100}→Ala and Ser^{100C}→Thr) into the DH570 HCDR3 amino acid sequence to mimic the HCDR3 sequence of DH570.IA47. This antibody mutant, DH570.Mut58 Fab, exhibited a fivefold increase in affinity [dissociation constant (K_d) = 83.7 and 17.8 nM for DH570 and DH570.Mut58, respectively] for MPER peptide-liposomes, largely due to an increased association rate [(k_a) = 2.87×10^4 and 12.9×10^4 M^{-1} s^{-1} for DH570 and DH570.Mut58 Fabs, respectively] (Fig. 5, A to C). Additionally, the dissociation rate of DH570.Mut58 Fab remained unchanged when compared to the original DH570 Fab (Fig. 5C). This faster association rate of DH570.Mut58 was associated with the ability to neutralize for HIV tier 1 clade B isolate W61D in the TZM-bl assay (Fig. 5D). Thus, a member of the DH570 lineage, with only two amino acid exchanges, could achieve heterologous HIV neutralization in the TZM-bl neutralization assay without FcγRI assistance.

DISCUSSION

Here, we demonstrate that germline knock-in mice expressing precursors of bnAb 2F5 showed B cell deletion in the bone marrow prevaccination, and the anergic bnAb precursors that survived in the periphery could be partially rescued, become activated, and clonally expand by immunization with MPER peptide-liposomes (Fig. 1D). Vaccination of rhesus macaques indicated that an alternative, if imperfect, solution to tolerance control of 2F5-like B cell expansion could develop by allowing clone DH570 to be induced, in which antibodies neutralized HIV, but only in TZM-bl $CD4^+$ cells that coexpressed FcγRI. DH570 antibodies neutralized tier 2 HIV in $FcγRI^+$ cultured monocytes, suggesting that DH570 antibodies may be able to prevent monocyte/macrophage infection in vivo but would be ineffective in preventing transmission to $CD4^+$ T cells.

Our previous work has demonstrated that kynureninase is involved in mediating negative selection for MPER bnAbs (11, 17). Here, we show that the immunization regimen broke tolerance to kynureninase and, in doing so, induced antibodies to the gp41 MPER DKW bnAb epitope (fig. S1). Here, our current study demonstrates that a second mediator of tolerance control is lipid binding, and this control is mediated through limitation of antibody CDR3 hydrophobicity.

One concern is the possible lack of T cell help preventing bnAb development. Here, we found in the neutralizing clonal lineage DH570 that all naturally isolated macaque antibodies were class-switched as IgG antibodies. The range of V_H nucleotide mutations in the clone ranged from 7 to 21.3% (Fig. 2 and table S3). Thus, in the setting of vaccinated macaques, evidence of a T-dependent response for the neutralizing clonal lineage was present with class switching of the neutralizing clone DH570 to IgG and accumulation of considerable V_H nucleotide mutations.

Of critical importance, we observed a ceiling of affinity maturation in the DH570 clonal lineage to the immunogen, where additional accumulation of mutations after the most potent neutralizing antibody in the clone (IA47) led to a loss of lipid insertion potential, a loss of affinity maturation, and subsequently reduced neutralization potency and breadth. This phenomenon is reminiscent of a ceiling effect limiting association rates of easy-to-induce antibodies during affinity maturation of antibodies against vesicular stomatitis virus (40, 41), whereas O'Keefe *et al.* (42) reported a ceiling of affinity maturation for hen egg lysozyme antibodies. We hypothesize that tolerance mechanisms in the germinal center were responsible for lowering the kinetic rate ceiling for gp41-targeted neutralizing antibodies by primarily selecting against B cells having BCRs with the capacity to effectively insert into lipids, and thus precluded the DH570 clonal lineage from developing the fast association rates of membrane binding of the 2F5 bnAb.

The reversal of affinity maturation for MPER peptide-liposomes with increasing maturation from antibody IA47 to DH570.20 and DH570.21 is remarkable and emphasizes the poorly understood capacity of germinal centers to select BCRs with lowered affinity for antigen in the presence of continued vaccination (17, 43, 44). The phenotype of reversion of binding affinity from autoreactivity to lipids with the accumulation of additional antibody mutations is similar to what has been described in mice for reversions away from autoreactivity to proteins (17, 44). CD4 T follicular helper (T_{fh}) cells are the drivers of affinity maturation in germinal centers (45, 46), and in mature 2F5 bnAb knock-in mice, MPER peptide-liposome–driven T cell helps select for non-MPER and nonneutralizing antibodies (17). Thus, our data raise the hypothesis that during continued immunization with MPER peptide-liposomes in macaques, T_{fh} cells in germinal centers may be driving antibody specificities away from lipid reactivity and therefore away from bnAb activity.

That we were able to improve the DH570 antibody association rate by making two HCDR3 amino acid mutations to increase the lipid insertion potential supports the hypothesis that, in the absence of tolerance constraints, affinity maturation can extend beyond the association rate ceiling. Furthermore, traversing beyond this association rate ceiling enabled the DH570 mutant antibody to achieve neutralization in the TZM-bl assay without assistance from

FcγRI, albeit with limited potency and breadth. Thus, the association rate ceiling control mechanism is hypothesized to be a limitation of the degree of hydrophobicity of the BCR HCDR3 because B cells expressing BCRs with hydrophobic HCDR3s are known to be deleted by tolerance controls (47), even though they are required for 2F5-like antibodies to neutralize HIV (13, 27).

Our study has limitations in that multiple immunogens and immunizations were associated with the appearance of the DH570 neutralizing clonal lineage. New studies will be required to determine whether the MPER peptide-liposome alone can induce such lineages. Moreover, the nature of the adjuvant required in humans will need to be determined. Such a study is currently under design for immunization of the MPER peptide-liposome in humans in a phase 1 clinical trial.

That bnAbs isolated from infected individuals can break through the association rate ceiling raises the hypothesis that in some HIV-infected individuals, tolerance controls are perturbed, allowing gp41 bnAb lineages to develop. It is encouraging that vaccination of macaques generated antibodies that could approach the specificity of gp41 bnAbs. It is hoped that in humans, immunization with the MPER peptide-liposome, an immunogen designed specifically for human bnAb UA antibody binding, will be more effective at driving neutralizing bnAb lineages. Iterative modifications of immunogen regimens will likely be needed to drive desired but disfavored B cell lineages to neutralization breadth. Finally, our data raise the hypothesis that vaccination with regimens designed to transiently dampen immune tolerance controls may also be required to raise the ceiling on affinity maturation to that of gp41 MPER-targeted bnAbs.

MATERIALS AND METHODS

Study design

The objective of this study was to profile the antibody repertoire in gp41 bnAb V_H and V_L knock-in mice and in outbred rhesus macaques after vaccination with HIV immunogens designed to engage the UA of a gp41 bnAb. The number of animals and their immunization regimens are provided below. The study was not blinded and randomization was not used in data collection or processing. For replicated neutralization assays where multiple batches of a produced antibody were used, we included neutralization data for the antibody from the antibody batch with the most robust neutralization capacity to ensure consistent antibody functionality within the batch. The number of replicates performed for each experiment is included in the figure legends.

2F5 dKI mouse models and immunization strategy

2F5 germline/UA dKI mice were generated on the C57BL/6 background on the basis of the techniques previously described to engineer the 2F5 original (mature) dKI model (22, 23). Briefly, 2F5 UA $V_HD_HJ_H^{+/+}$ KI mice were first generated by knocking in the published VDJ rearrangement of the inferred UA #1 (higher affinity to MPER epitope) allelic variant (26), using the previously described murine heavy chain locus targeting constructs and strategies (23). In parallel, recombinant embryonic stem cells bearing the murine κ locus-targeted

inferred 2F5 UA $V_\kappa J_\kappa$ rearrangement sequence (26) were used to derive 2F5 UA $V_\kappa J_\kappa^{+/+}$ mice on the basis of previously published methods (22). Finally, 2F5 UA $V_H D_H J_H^{+/+}$ and $V_\kappa J_\kappa^{+/+}$ mice were repeatedly crossbred to generate fully homozygous 2F5 UA dKI mice (22).

For all immunizations with 2F5 dKI models or control (wild-type B6) mice, a minimum of three mice per immunization group were used. All mice were 8 to 12 weeks old at the start of the immunization study and were housed in the Duke University Vivarium in a pathogen-free environment with 12-hour light/dark cycles at 20° to 25°C in accordance with all the Duke University Institutional Animal Care and Use Committee (IACUC)–approved animal protocols. Mice were immunized six times with TLR agonist–MPER peptide-liposome conjugates [25 μg of MPER 656-GTH1 peptide and 10 μg of monophosphoryl lipid A (MPLA)], as described (17) through intraperitoneal injections (200 μl) administered every 14 days. Blood samples were collected for isolation of sera 10 days after each immunization.

Calcium flux analysis for dKI models

After splenocytes were harvested, B cells were enriched using a mouse Pan-B Cell Isolation Kit (STEMCELL) according to the manufacturer's instructions. Enriched pan-B cells were stained by LIVE/DEAD Fixable Yellow Dead Cell Stain Kit (Thermo Fisher Scientific) and the cell surface makers anti–B220-BV711 and anti-CD93-APC (allophycocyanin) for 30 min. Prestained B cells were loaded with Fluo-4 through thorough washes in Hanks' balanced salt solution (HBSS), followed by mixing with equal volumes of 2× Fluo-4 Direct calcium reagent loading solution (Fluo-4 Direct Calcium Assay Kits, Thermo Fisher Scientific). After sequential 30-min incubations at 37°C and room temperature, cells were washed and resuspended in calcium-containing HBSS and incubated at room temperature for 5 min before being activated by anti-IgM F(ab')2 (25 μg/ml; SouthernBiotech). Fluo-4 MFI data for transitional ($B220^+$ $CD93^+$) B cells were acquired on a BD LSR II flow cytometer and analyzed by FlowJo software.

Enzyme-linked immunosorbent assays for 2F5 dKI models

Total Ig and MPER (2F5 neutralization epitope peptide; SP62)–specific serum antibody concentrations in age- and gender-matched 2F5 mature dKI, 2F5 UA dKI, and B6 mice were determined by enzyme-linked immunosorbent assays (ELISAs), as described (17,20,22). Briefly, purified mouse IgM (λ isotype) and IgG1 (κ isotype) were used as standard curves to measure total IgM and total IgG mouse antibody concentrations. Recombinant chimeric 2F5 mAb [human 2F5 V_H and mouse Cγ1 + human 2F5 V_κ and mouse C_κ (22)] was used as a reference standard to measure MPER-specific (that is, against plate-bound SP62) IgG concentrations; similarly, V3-1.4 [an m2F5 IgM antibody (20)] was used as a reference standard to measure MPER-specific IgM concentrations. Alkaline phosphatase (AP)–conjugated goat anti-mouse IgG and IgM antibodies (SouthernBiotech) were used as secondary antibodies.

Mouse B cell phenotypic analysis by flow cytometry

Flow cytometric analysis was performed as described (17, 20, 22). Briefly, single-cell suspensions from spleen and bone marrow were isolated from naïve and immunized 2F5

mature and 2F5 UA dKI mice; wild-type naïve C57BL/6 mice were used as controls. A total of 10 cells were suspended in fluorescence-activated cell sorting (FACS) buffer containing 1× phosphate-buffered saline (pH 7.2), 3% fetal bovine serum (Sigma-Aldrich), and 0.01% sodium azide, and B cells were stained with premixed combinations of fluorochrome-labeled mAbs at titration-determined optimal concentrations. Total B cells were gated as singlet, live, $CD19^+$, and/or $B220^+$ lymphocytes. All antibodies were from BD Biosciences unless otherwise stated. Primary labeled mAbs used were Pacific Blue, allophycocyanin, or Texas Red-conjugated anti-B220 (clone RA3–6B2), phycoerythrin (PE)–Cy7 anti-CD19, fluorescein isothiocyanate (FITC)–conjugated anti-IgD (clone 11–26), FITC-conjugated anti-IgG2b (clone R12-3), FITC-, allophycocyanin-, or PE-Cy7–conjugated anti-IgM (clone 15F9), PE-conjugated anti-CD21, and PE-Cy7–labeled anti-CD23 (eBioscience). Flow cytometric analysis of B cell reactivity for the MPER 2F5 epitope was performed similarly using single-cell splenocyte suspensions from naïve and immunized 2F5 mature and 2F5 UA dKI mice that were stained with MPER (SP62) tetramers, also as previously described (17, 22, 48). IgG2b- and IgM-specific analysis was performed using an intracellular staining protocol based on the BD Cytofix/Cytoperm fixation/permeabilization method. Representative gating strategies are shown in fig. S10.

Production of rVV expressing JRFL gp140

rVVs containing a codonoptimized JRFL gp140 gene (24) were generated and purified as described (49). The recombinant rVV-JRFL gp140 was confirmed by polymerase chain reaction (PCR) and DNA sequencing analysis and stocked at −80°C until use. Plaque-forming units (PFU) of each batch of rVVs were determined in BSC-1 cells as described (49).

Preparation of deglycosylated JRFL gp140

Natively deglycosylated recombinant JRFL gp140 (Deg JRFL gp140) was prepared by using peptide *N*-glycosidase F (PNGase F) (New England Biolabs) as described (24). The natively deglycosylated JRFL gp140 protein was confirmed by SDS–polyacrylamide gel electrophoresis and Western blot assay with MPER-reactive antibodies 2F5 and 4E10 and then stored at −80°C until use.

Adjuvant production

The adjuvant with oil and TLR agonists, LASTS-CR, was developed as described (50) and used in rhesus macaque immunizations with Deg JRFL gp140 protein. MPLA (Avanti Polar Lipids), R848 (InvivoGen), and oligonucleotide CpG (oCpG) with the sequence of 5′-TCGTC-GTTTCGTCGTTTTGTCGTT-3′ (ODN10103; The Midland Certified Reagent Co.) were added into Span85/Tween80/squalene with the final concentration of 200 μg/ml, 1 mg/ml, and 6.67 mg/ml, respectively, to make the adjuvant formulation LASTS-CR.

Rhesus macaques and immunization strategy

Four healthy, adult (one female and three males) Chinese-origin rhesus macaques were housed at BIOQUAL Inc. Macaques were immunized with a total dose of 10^9 PFU of rVV-JRFL gp140 at two sites each intramuscularly and intradermally (250 μl each site) at day 0.

Animals were then vaccinated with 100 μg of deglycosylated JRFL gp140 (83.3 μg/ml) in the presence of the adjuvant of LASTS-CR through mucosa: intranasal (500 μl), sublingual (500 μl), and tonsillar (200 μl) at week 8. Animals were boosted with 349.8 μg of adjuvant-containing (MPLA and R848) MPER peptide-liposomes (51) (291.5 μg/ml) in the presence of ODN10103 (final concentration of 6.67 mg/ml) through mucosa: intranasal (500 μl), sublingual (500 μl), and tonsillar (200 μl) at weeks 12, 16, 20, and 24. At weeks 32 and 36, the monkeys were boosted with 100 mg of deglycosylated JRFL gp140 (100 μg/ml) in the presence of the adjuvant of LASTS-CR at four sites intramuscularly (250 μl each site). The animals were then boosted with 1000 μg of adjuvant-containing MPER peptide-liposomes per animal (345 μg/ml) by four sites intramuscularly (750 μl each site) at weeks 41, 45, 50, 88, 92, 129, 135, 142, and 148. Blood was collected at preimmunization and 2 weeks after immunization for each immunization.

Flow cytometry macaque memory B cell single-cell sorting

MPER-specific memory B cells of macaque R585 and R584 were sorted by flow cytometry as described (30). Briefly, 1×10^7 PBMCs were stained with B cell antibody panel: CD14 (BV570), CD3 (PerCP-Cy5.5), CD20 (FITC), CD27 (APC-Cy7), and IgD (PE) (BD Biosciences) and Alexa Fluor 647 and Brilliant Violet 421–tagged MPER.03 peptides (KKKNEQELLELDKWASLWNWFDITNWLWYIRKKK). HIV gp41– specific memory B cells were gated as $CD3^-CD14^-CD20^+CD27^+sIgD^-MPER.03\ (AF647)^+$ $MPER.03\ (BV421)^+$ and sorted into 96-well PCR plates containing 20 μl of reverse transcription reaction buffer that included 5 μl of 5× first-strand complementary DNA (cDNA) buffer, 1.25 μl of dithiothreitol, 0.5 μl of RNaseOUT (Life Technologies), 0.0625 μl of Igepal (Sigma-Aldrich), and 13.25 μl of ultrapure deionized water (Life Technologies). Representative gating strategies are shown in fig. S11.

Sequencing and expression of rhesus macaque memory B cell V_HDJ_H and V_LJ_L genes

Rhesus macaque V_HDJ_H and V_LJ_L segments were isolated by single-cell reverse transcription PCR (RT-PCR) using the method as described (52). The isolated V(D)J gene fragments were used for the construction of linear expression cassettes for production of recombinant mAbs in 293T cells in small scale (53).

Expression of purified IgG1 recombinant mAbs

V(D)J gene fragments were de novo synthesized and cloned (GenScript) into the plasmids containing rhesus IgG1/IgK/IgL constant regions. Recombinant mAbs were produced in 293F cells (Life Technologies) by cotransfection with plasmids expressing the Ig heavy and light chain genes and were purified from the culture supernatant by protein A column chromatography. For generation of UCA and IA antibodies, inferred heavy chains were paired with light chains from the closest observed mature antibody in the lineage (UCA1). An additional UCA was made for DH570, referred to as DH570.UCA2, comprised of the inferred heavy chain paired with the light chain of DH570.7, the closest member in branch I (the branch of the DH570 lineage with the most neutralizing members). In the text, the term UCA refers to data from neutralization and binding assays with UCA2. The same assays were performed with UCA1 and yielded comparable results.

Clonal lineage determination and inference of UCAs

The software program Cloanalyst (54–56) was used to annotate isolated V_HDJ_H and V_LJ_L sequences with immunogenetic information as well as to test for clonal lineage membership, infer UCAs, and reconstruct phylogenetic trees of clonal lineages, as described (7, 9). Phylogenetic trees were reconstructed from heavy chains only. Note that the term UCA is used when inference was performed using multiple observed clonal members. When inference was performed with only a single observed antibody, the term UA is used.

Lipid insertion propensity

Lipid insertion propensity scores were calculated using the MPEx (Membrane Protein Explorer) software program (57) as a sum of ΔG_{wif}, the free energy of transfer of an amino acid from water to POPC interface (37), over all amino acids in the HCDR3 and/or LCDR3 where CDR amino acid positions were defined structurally using the DH570/MPER peptide complex structure (HCDR3, LFQPNGFSFTLTSYW; LCDR3, QQYISLPPT). Scores were calculated for all CDRs individually, and the most statistically significant discriminator of neutralization capacity for the DH570 clone was found to be the sum of HCDR3 and LCDR3 scores [$P < 0.01$, Wilcoxon-Mann-Whitney test with Benjamini-Hochberg (58) false discovery rate correction].

Rhesus mAb binding and epitope mapping

Rhesus macaque serum and recombinant mAbs were screened by ELISA (59) for binding specificities to a panel of HIV Envs (JRFL gp140 and MN gp41), recombinant HIV Env cores [GCN4 gp41-inter (33), gp41-6HB (60), and 5HelixH6 (60)], biotinylated MPER peptides including MPER03 (KKKNEQELLELDKWASLWNWFDITN-WLWYIRKKK-biotin), 2F5 epitope SP62 (QQEKNEQELLELDKWASLWN-biotin), 4E10/10E8 epitope peptide (SLWNWFNITNWLWYIK-biotin), and autoantigens [kynureninase (includes DKW) and kynureninase mutant (includes EKW) (11)]. AP-conjugated goat anti-human Ig (H + L) antibody (SouthernBiotech) was used for secondary detection. mAb epitope mapping was confirmed by surface plasmon resonance (SPR).

Rectal HIV-1 IgG

HIV-specific IgG was measured by a binding antibody multiplex assay (61,62), and IgG concentration was determined by ELISA from fluid recovered from rectal wecks of macaques 584 and 585. 2F5 peptide tetramer–specific mucosal IgG was reported as specific activity, which equals 2F5 mAb concentration equivalent (2F5 mAb ng/ml equiv)/total rhesus IgG (μg/ml).

Polyreactivity analysis of antibodies

The polyreactivity of rhesus mAbs was assessed with the AtheNA Multi-Lyte System (ZEUS Scientific) and HEp-2 cells immunofluorescence assay (Inverness Medical Professional Diagnostics) as described (63). DH570, DH570.IA47, and DH570.33 were tested for the reactivity with human host cellular antigens using ProtoArray 5 microchip (Life Technologies) as described (11).

Lipid and MPER liposome binding

Lipid binding of mAbs to synthetic liposomes {POPC, PCPS (POPC:POPS at 25:75 molar ratio), PCCLP [POPC: cardiolipin (Avanti Polar Lipids) at 25:75 molar ratio]} was measured by SPR assays on a BIAcore 3000 instrument, and data analyses were performed with BIAevaluation 4.1 software (Biacore/GE Healthcare) as described (64). MPER liposomes, without any adjuvant, were prepared using the same method as the MPER liposome immunogen described above. Antibody-binding kinetic rate constants (k_a and k_d) were measured by Bio-Layer Interferometry (BLI, ForteBio Octet RED96) measurements. The BLI assay was performed using APS (aminopropylsilane) sensors (ForteBio) to capture MPER liposomes and dipped into varying concentrations of antibodies after blocking of lipid-anchored sensors in bovine serum albumin (0.1%). Rate constants were calculated by curve fitting analyses (1:1 Langmuir model) of binding responses with a 10-min association and 15-min dissociation interaction time.

Neutralization assays

The neutralizing activity of rhesus serum samples and purified mAbs was detected against a panel of HIV isolates (HXB2, W61D, JRFL, SC422661.8, WITO4160.33, and MuLV as negative control) in both TZM-bl (65) and TZM-bl/FcγRI cells (31). Samples were tested at threefold dilution starting at 1:20 and ending at 1:43,740. The starting concentration of mAbs was 50 to 100 μg/ml. IC_{50} is calculated as the concentration in which 50% of virus was neutralized and units are reported as either reciprocal dilution for plasma samples or μg/ml for mAbs. Any IC_{50} values greater than the starting concentration were set equal to the starting concentration before calculating median values.

Time course of neutralization assay

The time course of neutralization of 2F5, DH570, and DH570.IA47 mAbs against HIV isolates W61D (TCLA) and SC422661 was measured in a synchronized post-attachment pseudotyped neutralization assay as described (32, 34, 35). Inhibitory concentration of either 2F5 (2.5 μg/ml in both TZM-bl and TZM-bl/FcγRI assays against W61D; 50 μg/ml in TZM-bl, 12.5 μg/ml in TZM-bl/FcγRI assay against SC422661) or DH570 mAbs (50 μg/ml in both TZM-bl and TZM-bl/FcγRI assays against W61D and SC422661) was added at different time intervals (0, 10, 20, 40, 60, 120, 180, and 240 min) to TZM-bl/FcγRI cells prebound to viruses. Luciferase activity assay was performed 48 hours after infection.

Next-generation sequencing

Total RNAs were extracted by the RNeasy Mini Kit (Qiagen) using the protocol recommended by the manufacturer from PBMCs collected at weeks 16, 24, 92, and 150 from R585 rhesus macaque and used to generate cDNA amplicons for NGS. RT-PCR reactions to generate Ig V(D)J cDNAs were performed by using a modified protocol as described (52). RT reactions were first performed in 30-μl reaction mixture with 5-μl RNA/reaction and a set of rhesus IgA, IgG, IgD, and IgM constant region–specific primers at a final concentration of 2 μM by using SuperScript III Reverse Transcriptase (Life Technologies). After cDNA synthesis, IGHV1-IGHV7 genes were amplified by PCR using the IGHV primers (V_H1/7A, V_H1/7B, V_H2, V_H3A, V_H3B, V_H3C, V_H3D, V_H4A, V_H4B,

V_H5, and V_H6) (at a final concentration of 0.2 nM each) individually pairing with the mixture of reverse primers of rhesus IgA, IgG, IgD, and IgM (at a final concentration of 0.12 nM each) (SI: rhesus macaque NGS primer list). Platinum Taq DNA Polymerase High Fidelity (Life Technologies) was used in the PCR reaction: 1.25 U of Platinum Taq DNA Polymerase High Fidelity, 5 μl of RT reaction products, 5 μl of 10× High-Fidelity Buffer, 1 μl of 10 mM deoxynucleotide triphosphates (dNTPs), 2.5 μl of 50 mM $MgCl_2$, 1 μl of 10 μM IGHV primer, and 2.4 μl of mixture of IgA, IgD, IgG, and IgM constant region primers (10 μM each). PCR was performed at 94°C × 2 min followed by 25 cycles of 94°C × 15 s, 60°C × 30 s, and 68°C × 30 s, and one cycle at 68°C × 10 min. PCR products were purified using QIAquick PCR Purification Kit (Qiagen) and eluted into 50-μl Ultrapure DNase/RNase-Free Distilled Water. Bar codes and Illumina pyrosequencing tags were added to the purified amplicons by PCR for a total of 11 cycles in 50 μl of reaction mixture including 1.25 U of Platinum Taq DNA Polymerase High Fidelity, 5 μl of the purified amplicon, 5 μl of 10× High-Fidelity Buffer, 1 μl of 10 mM dNTPs, 2.0 μl of 50 mM $MgCl_2$, and 10 μl of Nextera Index Kit bar code–tagged primers (5 μl each) (Illumina). PCR was performed at 94°C × 2 min followed by three cycles of 94°C × 15 s, 55°C × 30 s, and 68°C × 30 s, eight cycles of 94°C × 15 s, 60°C × 30 s, and 68°C × 30 s, and one cycle at 68°C × 10 min. The bar-coded amplicons were individually purified with QIAquick Gel Extraction Kit (Qiagen) and eluted with 25 μl of UltraPure DNase/RNase-Free Distilled Water. The purified individually bar-coded amplicons were then pooled together on the basis of equal volume and quantified on StepOnePlus Real-Time PCR System (Life Technologies) using the KAPA SYBR FAST qPCR kit (Kapa Biosystems). Pooled amplicons (5 μl at 4 μM) were denatured with 5 μl of 0.2 N NaOH and mixed with 990 μl of hybridization buffer (Illumina). Five microliters of 4 nM PhiX control DNA (Illumina) was also denatured with 5 μl of 0.2-N NaOH and mixed with 990 μl of hybridization buffer. A total of 650 μl of the denatured sample pool was mixed with 350 μl of the denatured PhiX. A total of 600 μl of the mixture was then loaded to Illumina MiSeq kit V3 (2 × 300 base pairs; Illumina) for sequencing.

Paired-end sequences generated by NGS using MiSeq were merged using FLASH (fast length adjustment of short reads) and quality control– filtered (Q score >30 for >95% of sequence) using the FASTX-Toolkit. V_HDJ_H rearrangements were inferred and tested for clonal relatedness using Cloanalyst software suite as described previously (7). V_HDJ_H rearrangements were computationally evaluated for meeting the following 2F5-like criteria: triple Asp in HCDR2, double Arg in base of HCDR3, Leu-Phe in middle of HCDR3, and two or more Pro in HCDR3.

Crystallography

The Fabs of DH570, DH570.4, and DH570.9 were generated by cotransfecting the plasmids coding IgH Fab chain and IgK chain into 293i cells (Life Technologies) and purified with protein A agarose (Thermo Scientific) as described (9). All crystals were grown at a temperature of 20°C in SBS format plates. Unliganded DH570 Fab was crystallized at a concentration of 35.9 mg/ml over a reservoir of 0.1 M MES (pH 6.0), 14% PEG 4000. Unliganded DH570.4 Fab was crystallized at a concentration of 15.0 mg/ml over a reservoir of 0.2 M NaI, 20% PEG 3350. Unliganded DH570.9 Fab was crystallized at a concentration of 14.5 mg/ml over a reservoir of 0.1 M bis-tris (pH 6.5), 20% PEG 1500. A $gp41_{660–670}$

peptide (11-mer; Ac-LLELDKWASLW-NH2) (66) was commercially synthesized, and the complex of DH570 Fab with $gp41_{660–670}$ peptide was grown at a concentration of 20 mg/ml total protein over a reservoir of 24% PEG 1500, 20% glycerol with microseeding using the aforementioned unliganded DH570 Fab crystals.

All crystals were cryoprotected by supplementing mother liquor with ethylene glycol and then flash-frozen in liquid nitrogen. Diffraction data were collected either in-house on a Rigaku 007 HF instrument generating copper Kα radiation or at SER-CAT (Southeast Regional Collaborative Access Team) with an incident beam of 1 Å in wavelength. Data sets were reduced in HKL-2000 (67). Matthews analysis suggested one Fab molecule or Fab-peptide complex in the asymmetric unit of each structure (68). The unliganded DH570 Fab structure was phased by molecular replacement in PHENIX (69) using source models chosen by high sequence homology: the heavy chain of rhesus 2.5B Fab (70) and light chain of a vascular endothelial growth factor–blocking Fab (71). Rebuilding and real-space refinements were done in Coot (72) with reciprocal-space refinements in PHENIX (73) and validations in MolProbity (74).

Statistical analysis

Statistical analysis was performed in SAS version 9.4 (SAS Institute). All statistical tests performed were Wilcoxon-Mann-Whitney tests with Benjamini-Hochberg (58) false discovery rate correction for multiple testing. The P values for Fig. 1 are listed in table S8. $*P < 0.05$; $**P < 0.01$; $***P < 0.001$.

Supplementary Material

Refer to Web version on PubMed Central for supplementary material.

Acknowledgments

We thank R. Glenn Overman, D. Beaumont, and M. Donathan for technical assistance for mucosal antibody assays; K. Anasti for performing BLI experiments and data analysis for kinetic rate measurements; F. Jaeger for SPR analysis of antibody epitope mapping; S.-M. Xia and M. Cooper for neutralization assays; A. Wang for computational analysis; A. A. Allen, L. C. Armand, D. J. Marshall, and J. F. Whitesides for flow cytometric experiments on rhesus macaques. Data were collected at SER-CAT 22-ID (or 22-BM) beamline at the Advanced Photon Source, Argonne National Laboratory. Supporting institutions may be found at www.ser-cat.org/members.html. The use of the Advanced Photon Source was supported by the U.S. Department of Energy Office of Science and Office of Basic Energy Sciences under contract no. W-31-109-Eng-38.

Funding: This work was supported by the Center for HIV/AIDS Vaccine Immunology and Immunogen Discovery (CHAVI-ID; UMI-AI100645) grant from NIH/National Institute of Allergy and Infectious Diseases/Division of AIDS and Collaboration for AIDS Vaccine Discovery grants to B.F.H. and P.D.G. from the Bill & Melinda Gates Foundation.

REFERENCES AND NOTES

1. Mascola JR, Haynes BF. HIV-1 neutralizing antibodies: Understanding nature’s pathways. Immunol. Rev. 2013; 254:225–244. [PubMed: 23772623]
2. Burton DR, Mascola JR. Antibody responses to envelope glycoproteins in HIV-1 infection. Nat. Immunol. 2015; 16:571–576. [PubMed: 25988889]
3. Dosenovic P, von Boehmer L, Escolano A, Jardine J, Freund NT, Gitlin AD, McGuire AT, Kulp DW, Oliveira T, Scharf L, Pietzsch J, Gray MD, Cupo A, van Gils MJ, Yao K-H, Liu C, Gazumyan A, Seaman MS, Björkman PJ, Sanders RW, Moore JP, Stamatatos L, Schief WR, Nussenzweig MC.

Immunization for HIV-1 broadly neutralizing antibodies in human Ig knockin mice. Cell. 2015; 161:1505–1515. [PubMed: 26091035]

4. Jardine JG, Ota T, Sok D, Pauthner M, Kulp DW, Kalyuzhniy O, Skog PD, Thinnes TC, Bhullar D, Briney B, Menis S, Jones M, Kubitz M, Spencer S, Adachi Y, Burton DR, Schief WR, Nemazee D. Priming a broadly neutralizing antibody response to HIV-1 using a germline-targeting immunogen. Science. 2015; 349:156–161. [PubMed: 26089355]
5. Sanders RW, van Gils MJ, Derking R, Sok D, Ketas TJ, Burger JA, Ozorowski G, Cupo A, Simonich C, Goo L, Arendt H, Kim HJ, Lee JH, Pugach P, Williams M, Debnath G, Moldt B, van Breemen MJ, Isik G, Medina-Ramírez M, Back JW, Koff WC, Julien J-P, Rakasz EG, Seaman MS, Guttman M, Lee KK, Klasse PJ, LaBranche C, Schief WR, Wilson IA, Overbaugh J, Burton DR, Ward AB, Montefiori DC, Dean H, Moore JP. HIV-1 neutralizing antibodies induced by native-like envelope trimers. Science. 2015; 349:aac4223. [PubMed: 26089353]
6. Hu JK, Crampton JC, Cupo A, Ketas T, van Gils MJ, Sliepen K, de Taeye SW, Sok D, Ozorowski G, Deresa I, Stanfield R, Ward AB, Burton DR, Klasse PJ, Sanders RW, Moore JP, Crotty S. Murine antibody responses to cleaved soluble HIV-1 envelope trimers are highly restricted in specificity. J. Virol. 2015; 89:10383–10398. [PubMed: 26246566]
7. Williams WB, Liao H-X, Moody MA, Kepler TB, Alam SM, Gao F, Wiehe K, Trama AM, Jones K, Zhang R, Song H, Marshall DJ, Whitesides JF, Sawatzki K, Hua A, Liu P, Tay MZ, Seaton KE, Shen X, Foulger A, Lloyd KE, Parks R, Pollara J, Ferrari G, Yu J-S, Vandergrift N, Montefiori DC, Sobieszczyk ME, Hammer S, Karuna S, Gilbert P, Grove D, Grunenberg N, McElrath MJ, Mascola JR, Koup RA, Corey L, Nabel GJ, Morgan C, Churchyard G, Maenza J, Keefer M, Graham BS, Baden LR, Tomaras GD, Haynes BF. Diversion of HIV-1 vaccine-induced immunity by gp41-microbiota cross-reactive antibodies. Science. 2015; 349:aab1253. [PubMed: 26229114]
8. McGuire AT, Hoot S, Dreyer AM, Lippy A, Stuart A, Cohen KW, Jardine J, Menis S, Scheid JF, West AP, Schief WR, Stamatatos L. Engineering HIV envelope protein to activate germline B cell receptors of broadly neutralizing anti-CD4 binding site antibodies. J. Exp. Med. 2013; 210:655–663. [PubMed: 23530120]
9. Liao H-X, Lynch R, Zhou T, Gao F, Alam SM, Boyd SD, Fire AZ, Roskin KM, Schramm CA, Zhang Z, Zhu J, Shapiro L, Comparative Sequencing NISC, Program L, Mullikin JC, Gnanakaran S, Hraber P, Wiehe K, Kelsoe G, Yang G, Xia S-M, Montefiori DC, Parks R, Lloyd KE, Scearce RM, Soderberg KA, Cohen M, Kamanga G, Louder MK, Tran LM, Chen Y, Cai F, Chen S, Moquin S, Du X, Joyce MG, Srivatsan S, Zhang B, Zheng A, Shaw GM, Hahn BH, Kepler TB, Korber BTM, Kwong PD, Mascola JR, Haynes BF. Co-evolution of a broadly neutralizing HIV-1 antibody and founder virus. Nature. 2013; 496:469–476. [PubMed: 23552890]
10. Haynes BF, Fleming J, St. Clair EW, Katinger H, Stiegler G, Kunert R, Robinson J, Scearce RM, Plonk K, Staats HF, Ortel TL, Liao H-X, Alam SM. Cardiolipin polyspecific autoreactivity in two broadly neutralizing HIV-1 antibodies. Science. 2005; 308:1906–1908. [PubMed: 15860590]
11. Yang G, Holl TM, Liu Y, Li Y, Lu X, Nicely NI, Kepler TB, Alam SM, Liao H-X, Cain DW, Spicer L, VandeBerg JL, Haynes BF, Kelsoe G. Identification of autoantigens recognized by the 2F5 and 4E10 broadly neutralizing HIV-1 antibodies. J. Exp. Med. 2013; 210:241–256. [PubMed: 23359068]
12. Liu M, Yang G, Wiehe K, Nicely NI, Vandergrift NA, Rountree W, Bonsignori M, Alam SM, Gao J, Haynes BF, Kelsoe G, Silvestri G. Polyreactivity and autoreactivity among HIV-1 antibodies. J. Virol. 2015; 89:784–798. [PubMed: 25355869]
13. Alam SM, Morelli M, Dennison SM, Liao H-X, Zhang R, Xia S-M, Rits-Volloch S, Sun L, Harrison SC, Haynes BF, Chen B. Role of HIV membrane in neutralization by two broadly neutralizing antibodies. Proc. Natl. Acad. Sci. U.S.A. 2009; 106:20234–20239. [PubMed: 19906992]
14. Alam SM, McAdams M, Boren D, Rak M, Scearce RM, Gao F, Camacho ZT, Gewirth D, Kelsoe G, Chen P, Haynes BF. The role of antibody polyspecificity and lipid reactivity in binding of broadly neutralizing anti-HIV-1 envelope human monoclonal antibodies 2F5 and 4E10 to glycoprotein 41 membrane proximal envelope epitopes. J. Immunol. 2007; 178:4424–4435. [PubMed: 17372000]

15. Chen J, Frey G, Peng H, Rits-Volloch S, Garrity J, Seaman MS, Chen B. Mechanism of HIV-1 neutralization by antibodies targeting a membrane-proximal region of gp41. J. Virol. 2014; 88:1249–1258. [PubMed: 24227838]
16. Sun Z-YJ, Oh KJ, Kim M, Yu J, Brusic V, Song L, Qiao Z, Wang J-h, Wagner G, Reinherz EL. HIV-1 broadly neutralizing antibody extracts its epitope from a kinked gp41 ectodomain region on the viral membrane. Immunity. 2008; 28:52–63. [PubMed: 18191596]
17. Verkoczy L, Chen Y, Zhang J, Bouton-Verville H, Newman A, Lockwood B, Scearce RM, Montefiori DC, Dennison SM, Xia S-M, Hwang K-K, Liao H-X, Alam SM, Haynes BF. Induction of HIV-1 broad neutralizing antibodies in 2F5 knock-in mice: Selection against membrane proximal external region-associated autoreactivity limits T-dependent responses. J. Immunol. 2013; 191:2538–2550. [PubMed: 23918977]
18. Guenaga J, Wyatt RT. Structure-guided alterations of the gp41-directed HIV-1 broadly neutralizing antibody 2F5 reveal new properties regarding its neutralizing function. PLOS Pathog. 2012; 8:e1002806. [PubMed: 22829767]
19. Dennison SM, Stewart SM, Stempel KC, Liao H-X, Haynes BF, Alam SM. Stable docking of neutralizing human immunodeficiency virus type 1 gp41 membrane-proximal external region monoclonal antibodies 2F5 and 4E10 is dependent on the membrane immersion depth of their epitope regions. J. Virol. 2009; 83:10211–10223. [PubMed: 19640992]
20. Chen Y, Zhang J, Hwang K-K, Bouton-Verville H, Xia S-M, Newman A, Ouyang Y-B, Haynes BF, Verkoczy L. Common tolerance mechanisms, but distinct cross-reactivities associated with gp41 and lipids, limit production of HIV-1 broad neutralizing antibodies 2F5 and 4E10. J. Immunol. 2013; 191:1260–1275. [PubMed: 23825311]
21. Zhang J, Alam SM, Bouton-Verville H, Chen Y, Newman A, Stewart S, Jaeger FH, Montefiori DC, Dennison SM, Haynes BF, Verkoczy L. Modulation of nonneutralizing HIV-1 gp41 responses by an MHC-restricted T_H epitope overlapping those of membrane proximal external region broadly neutralizing antibodies. J. Immunol. 2014; 192:1693–1706. [PubMed: 24465011]
22. Verkoczy L, Chen Y, Bouton-Verville H, Zhang J, Diaz M, Hutchinson J, Ouyang Y-B, Alam SM, Holl TM, Hwang K-K, Kelsoe G, Haynes BF. Rescue of HIV-1 broad neutralizing antibody-expressing B cells in 2F5 $V_H \times V_L$ knockin mice reveals multiple tolerance controls. J. Immunol. 2011; 187:3785–3797. [PubMed: 21908739]
23. Verkoczy L, Diaz M, Holl TM, Ouyang Y-B, Bouton-Verville H, Alam SM, Liao H-X, Kelsoe G, Haynes BF. Autoreactivity in an HIV-1 broadly reactive neutralizing antibody variable region heavy chain induces immunologic tolerance. Proc. Natl. Acad. Sci. U.S.A. 2010; 107:181–186. [PubMed: 20018688]
24. Ma B-J, Alam SM, Go EP, Lu X, Desaire H, Tomaras GD, Bowman C, Sutherland LL, Scearce RM, Santra S, Letvin NL, Kepler TB, Liao H-X, Haynes BF. Envelope deglycosylation enhances antigenicity of HIV-1 gp41 epitopes for both broad neutralizing antibodies and their unmutated ancestor antibodies. PLOS Pathog. 2011; 7:e1002200. [PubMed: 21909262]
25. Goodnow CC, Crosbie J, Jorgensen H, Brink RA, Basten A. Induction of self-tolerance in mature peripheral B lymphocytes. Nature. 1989; 342:385–391. [PubMed: 2586609]
26. Alam SM, Liao H-X, Dennison SM, Jaeger F, Parks R, Anasti K, Foulger A, Donathan M, Lucas J, Verkoczy L, Nicely N, Tomaras GD, Kelsoe G, Chen B, Kepler TB, Haynes BF. Differential reactivity of germ line allelic variants of a broadly neutralizing HIV-1 antibody to a gp41 fusion intermediate conformation. J. Virol. 2011; 85:11725–11731. [PubMed: 21917975]
27. Kim M, Sun Z-Y, Rand KD, Shi X, Song L, Cheng Y, Fahmy AF, Majumdar S, Ofek G, Yang Y, Kwong PD, Wang J-H, Engen JR, Wagner G, Reinherz EL. Antibody mechanics on a membrane-bound HIV segment essential for GP41-targeted viral neutralization. Nat. Struct. Mol. Biol. 2011; 18:1235–1243. [PubMed: 22002224]
28. Ofek G, Tang M, Sambor A, Katinger H, Mascola JR, Wyatt R, Kwong PD. Structure and mechanistic analysis of the anti-human immunodeficiency virus type 1 antibody 2F5 in complex with its gp41 epitope. J. Virol. 2004; 78:10724–10737. [PubMed: 15367639]
29. Zhang M-Y, Xiao X, Sidorov IA, Choudhry V, Cham F, Zhang PF, Bouma P, Zwick M, Choudhary A, Montefiori DC, Broder CC, Burton DR, Quinnan GV Jr, Dimitrov DS. Identification and characterization of a new cross-reactive human immunodeficiency virus type 1-neutralizing human monoclonal antibody. J. Virol. 2004; 78:9233–9242. [PubMed: 15308718]

30. Morris L, Chen X, Alam M, Tomaras G, Zhang R, Marshall DJ, Chen B, Parks R, Foulger A, Jaeger F, Donathan M, Bilska M, Gray ES, Abdool Karim SS, Kepler TB, Whitesides J, Montefiori D, Moody MA, Liao H-X, Haynes BF. Isolation of a human anti-HIV gp41 membrane proximal region neutralizing antibody by antigen-specific single B cell sorting. PLOS One. 2011; 6:e23532. [PubMed: 21980336]

31. Perez LG, Costa MR, Todd CA, Haynes BF, Montefiori DC. Utilization of immunoglobulin G Fc receptors by human immunodeficiency virus type 1: A specific role for antibodies against the membrane-proximal external region of gp41. J. Virol. 2009; 83:7397–7410. [PubMed: 19458010]

32. Shen X, Dennison SM, Liu P, Gao F, Jaeger F, Montefiori DC, Verkoczy L, Haynes BF, Alam SM, Tomaras GD. Prolonged exposure of the HIV-1 gp41 membrane proximal region with L669S substitution. Proc. Natl. Acad. Sci. U.S.A. 2010; 107:5972–5977. [PubMed: 20231447]

33. Frey G, Chen J, Rits-Volloch S, Freeman MM, Zolla-Pazner S, Chen B. Distinct conformational states of HIV-1 gp41 are recognized by neutralizing and non-neutralizing antibodies. Nat. Struct. Mol. Biol. 2010; 17:1486–1491. [PubMed: 21076402]

34. Dimitrov AS, Jacobs A, Finnegan CM, Stiegler G, Katinger H, Blumenthal R. Exposure of the membrane-proximal external region of HIV-1 gp41 in the course of HIV-1 envelope glycoprotein-mediated fusion. Biochemistry. 2007; 46:1398–1401. [PubMed: 17260969]

35. Gustchina E, Bewley CA, Clore GM. Sequestering of the prehairpin intermediate of gp41 by peptide $N36^{Mut(e,g)}$ potentiates the human immunodeficiency virus type 1 neutralizing activity of monoclonal antibodies directed against the N-terminal helical repeat of gp41. J. Virol. 2008; 82:10032–10041. [PubMed: 18667502]

36. Zhen A, Krutzik SR, Levin BR, Kasparian S, Zack JA, Kitchen SG. CD4 ligation on human blood monocytes triggers macrophage differentiation and enhances HIV infection. J. Virol. 2014; 88:9934–9946. [PubMed: 24942581]

37. Wimley WC, White SH. Experimentally determined hydrophobicity scale for proteins at membrane interfaces. Nat. Struct. Biol. 1996; 3:842–848. [PubMed: 8836100]

38. Ofek G, Zirkle B, Yang Y, Zhu Z, McKee K, Zhang B, Chuang G-Y, Georgiev IS, O'Dell S, Doria-Rose N, Mascola JR, Dimitrov DS, Kwong PD. Structural basis for HIV-1 neutralization by 2F5-like antibodies m66 and m66.6. J. Virol. 2014; 88:2426–2441. [PubMed: 24335316]

39. Northrup SH, Erickson HP. Kinetics of protein-protein association explained by Brownian dynamics computer simulation. Proc. Natl. Acad. Sci. U.S.A. 1992; 89:3338–3342. [PubMed: 1565624]

40. Foote J, Eisen HN. Kinetic and affinity limits on antibodies produced during immune responses. Proc. Natl. Acad. Sci. U.S.A. 1995; 92:1254–1256. [PubMed: 7877964]

41. Roost H-P, Bachmann MF, Haag A, Kalinke U, Pliska V, Hengartner H, Zinkernagel RM. Early high-affinity neutralizing anti-viral IgG responses without further overall improvements of affinity. Proc. Natl. Acad. Sci. U.S.A. 1995; 92:1257–1261. [PubMed: 7877965]

42. O'Keefe TL, Williams GT, Batista FD, Neuberger MS. Deficiency in CD22, a B cell-specific inhibitory receptor, is sufficient to predispose to development of high affinity autoantibodies. J. Exp. Med. 1999; 189:1307–1313. [PubMed: 10209047]

43. Haynes BF, Verkoczy L, Kelsoe G. Redemption of autoreactive B cells. Proc. Natl. Acad. Sci. U.S.A. 2014; 111:9022–9023. [PubMed: 24920593]

44. Sabouri Z, Schofield P, Horikawa K, Spierings E, Kipling D, Randall KL, Langley D, Roome B, Vazquez-Lombardi R, Rouet R, Hermes J, Chan TD, Brink R, Dunn-Walters DK, Christ D, Goodnow CC. Redemption of autoantibodies on anergic B cells by variable-region glycosylation and mutation away from self-reactivity. Proc. Natl. Acad. Sci. U.S.A. 2014; 111:E2567–E2575. [PubMed: 24821781]

45. Locci M, Havenar-Daughton C, Landais E, Wu J, Kroenke MA, Arlehamn CL, Su LF, Cubas R, Davis MM, Sette A, Haddad; International AIDS Vaccine Initiative Protocol C Principal , Investigators EK, Poignard P, Crotty S. Human circulating PD-1^{+}CXCR3CXCR5^{+} memory Tfh cells are highly functional and correlate with broadly neutralizing HIV antibody responses. Immunity. 2013; 39:758–769. [PubMed: 24035365]

46. Crotty S. T follicular helper cell differentiation, function, and roles in disease. Immunity. 2014; 41:529–542. [PubMed: 25367570]

47. Meffre E, Milili M, Blanco-Betancourt C, Antunes H, Nussenzweig MC, Schiff C. Immunoglobulin heavy chain expression shapes the B cell receptor repertoire in human B cell development. J. Clin. Invest. 2001; 108:879–886. [PubMed: 11560957]
48. Verkoczy L, Moody MA, Holl TM, Bouton-Verville H, Scearce RM, Hutchinson J, Alam SM, Kelsoe G, Haynes BF. Functional, non-clonal IgM^a-restricted B cell receptor interactions with the HIV-1 envelope gp41 membrane proximal external region. PLOS One. 2009; 4:e7215. [PubMed: 19806186]
49. Santra S, Liao H-X, Zhang R, Muldoon M, Watson S, Fischer W, Theiler J, Szinger J, Balachandran H, Buzby A, Quinn D, Parks RJ, Tsao C-Y, Carville A, Mansfield KG, Pavlakis GN, Felber BK, Haynes BF, Korber BT, Letvin NL. Mosaic vaccines elicit CD8$^+$ T lymphocyte responses that confer enhanced immune coverage of diverse HIV strains in monkeys. Nat. Med. 2010; 16:324–328. [PubMed: 20173754]
50. Moody MA, Santra S, Vandergrift NA, Sutherland LL, Gurley TC, Drinker MS, Allen AA, Xia S-M, Meyerhoff RR, Parks R, Lloyd KE, Easterhoff D, Alam SM, Liao H-X, Ward BM, Ferrari G, Montefiori DC, Tomaras GD, Seder RA, Letvin NL, Haynes BF. Toll-like receptor 7/8 (TLR7/8) and TLR9 agonists cooperate to enhance HIV-1 envelope antibody responses in rhesus macaques. J. Virol. 2014; 88:3329–3339. [PubMed: 24390332]
51. Dennison SM, Sutherland LL, Jaeger FH, Anasti KM, Parks R, Stewart S, Bowman C, Xia S-M, Zhang R, Shen X, Scearce RM, Ofek G, Yang Y, Kwong PD, Santra S, Liao H-X, Tomaras G, Letvin NL, Chen B, Alam SM, Haynes BF. Induction of antibodies in rhesus macaques that recognize a fusion-intermediate conformation of HIV-1 gp41. PLOS One. 2011; 6:e27824. [PubMed: 22140469]
52. Wiehe K, Easterhoff D, Luo K, Nicely NI, Bradley T, Jaeger FH, Dennison SM, Zhang R, Lloyd KE, Stolarchuk C, Parks R, Sutherland LL, Scearce RM, Morris L, Kaewkungwal J, Nitayaphan S, Pitisuttithum P, Rerks-Ngarm S, Sinangil F, Phogat S, Michael NL, Kim JH, Kelsoe G, Montefiori DC, Tomaras GD, Bonsignori M, Santra S, Kepler TB, Alam SM, Moody MA, Liao H-X, Haynes BF. Antibody light-chain-restricted recognition of the site of immune pressure in the RV144 HIV-1 vaccine trial is phylogenetically conserved. Immunity. 2014; 41:909–918. [PubMed: 25526306]
53. Liao H-X, Levesque MC, Nagel A, Dixon A, Zhang R, Walter E, Parks R, Whitesides J, Marshall DJ, Hwang K-K, Yang Y, Chen X, Gao F, Munshaw S, Kepler TB, Denny T, Moody MA, Haynes BF. High-throughput isolation of immunoglobulin genes from single human B cells and expression as monoclonal antibodies. J. Virol. Methods. 2009; 158:171–179. [PubMed: 19428587]
54. Cloanalyst. http://www.bu.edu/computationalimmunology/research/software/
55. Kepler TB. Reconstructing a B-cell clonal lineage. I. Statistical inference of unobserved ancestors [version 1; referees: 2 approved, 1 approved with reservations]. F1000Res. 2013; 2:103. [PubMed: 24555054]
56. Kepler TB, Munshaw S, Wiehe K, Zhang R, Yu J-S, Woods CW, Denny TN, Tomaras GD, Alam SM, Moody MA, Kelsoe G, Liao H-X, Haynes BF. Reconstructing a B-cell clonal lineage. II. Mutation, selection, and affinity maturation. Front. Immunol. 2014; 5:170. [PubMed: 24795717]
57. Snider C, Jayasinghe S, Hristova K, White SH. MPEx: A tool for exploring membrane proteins. Protein Sci. 2009; 18:2624–2628. [PubMed: 19785006]
58. Benjamini Y, Hochberg Y. Controlling the false discovery rate: A practical and powerful approach to multiple testing. J. R. Stat. Soc. B Met. 1995; 57:289–300.
59. Liao H-X, Bonsignori M, Alam SM, McLellan JS, Tomaras GD, Moody MA, Kozink DM, Hwang K-K, Chen X, Tsao C-Y, Liu P, Lu X, Parks RJ, Montefiori DC, Ferrari G, Pollara J, Rao M, Peachman KK, Santra S, Letvin NL, Karasavvas N, Yang Z-Y, Dai K, Pancera M, Gorman J, Wiehe K, Nicely NI, Rerks-Ngarm S, Nitayaphan S, Kaewkungwal J, Pitisuttithum P, Tartaglia J, Sinangil F, Kim JH, Michael NL, Kepler TB, Kwong PD, Mascola JR, Nabel GJ, Pinter A, Zolla-Pazner S, Haynes BF. Vaccine induction of antibodies against a structurally heterogeneous site of immune pressure within HIV-1 envelope protein variable regions 1 and 2. Immunity. 2013; 38:176–186. [PubMed: 23313589]
60. Root MJ, Kay MS, Kim PS. Protein design of an HIV-1 entry inhibitor. Science. 2001; 291:884–888. [PubMed: 11229405]
61. Yates NL, Stacey AR, Nolen TL, Vandergrift NA, Moody MA, Montefiori DC, Weinhold KJ, Blattner WA, Borrow P, Shattock R, Cohen MS, Haynes BF, Tomaras GD. HIV-1 gp41 envelope

IgA is frequently elicited after transmission but has an initial short response half-life. Mucosal Immunol. 2013; 6:692–703. [PubMed: 23299618]

62. Tomaras GD, Yates NL, Liu P, Qin L, Fouda GG, Chavez LL, Decamp AC, Parks RJ, Ashley VC, Lucas JT, Cohen M, Eron J, Hicks CB, Liao H-X, Self SG, Landucci G, Forthal DN, Weinhold KJ, Keele BF, Hahn BH, Greenberg ML, Morris L, Karim SS, Blattner WA, Montefiori DC, Shaw GM, Perelson AS, Haynes BF. Initial B-cell responses to transmitted human immunodeficiency virus type 1: Virion-binding immunoglobulin M (IgM) and IgG antibodies followed by plasma anti-gp41 antibodies with ineffective control of initial viremia. J. Virol. 2008; 82:12449–12463. [PubMed: 18842730]
63. Moody MA, Yates NL, Amos JD, Drinker MS, Eudailey JA, Gurley TC, Marshall DJ, Whitesides JF, Chen X, Foulger A, Yu JS, Zhang R, Meyerhoff RR, Parks R, Scull JC, Wang L, Vandergrift NA, Pickeral J, Pollara J, Kelsoe G, Alam SM, Ferrari G, Montefiori DC, Voss G, Liao HX, Tomaras GD, Haynes BF. HIV-1 gp120 vaccine induces affinity maturation in both new and persistent antibody clonal lineages. J. Virol. 2012; 86:7496–7507. [PubMed: 22553329]
64. Dennison SM, Anasti K, Scearce RM, Sutherland L, Parks R, Xia S-M, Liao H-X, Gorny MK, Zolla-Pazner S, Haynes BF, Alam SM. Nonneutralizing HIV-1 gp41 envelope cluster II human monoclonal antibodies show polyreactivity for binding to phospholipids and protein autoantigens. J. Virol. 2011; 85:1340–1347. [PubMed: 21106741]
65. Li M, Gao F, Mascola JR, Stamatatos L, Polonis VR, Koutsoukos M, Voss G, Goepfert P, Gilbert P, Greene KM, Bilska M, Kothe DL, Salazar-Gonzalez JF, Wei X, Decker JM, Hahn BH, Montefiori DC. Human immunodeficiency virus type 1 env clones from acute and early subtype B infections for standardized assessments of vaccine-elicited neutralizing antibodies. J. Virol. 2005; 79:10108–10125. [PubMed: 16051804]
66. Bird GH, Irimia A, Ofek G, Kwong PD, Wilson IA, Walensky LD. Stapled HIV-1 peptides recapitulate antigenic structures and engage broadly neutralizing antibodies. Nat. Struct. Mol. Biol. 2014; 21:1058–1067. [PubMed: 25420104]
67. Otwinowski A, Minor W. Processing of X-ray diffraction data collected in oscillation model. Methods Enzymol. 1997; 276:307–326.
68. Matthews BW. Solvent content of protein crystals. J. Mol. Biol. 1968; 33:491–497. [PubMed: 5700707]
69. Terwilliger TC, Grosse-Kunstleve RW, Afonine PV, Moriarty NW, Zwart PH, Hung L-W, Read RJ, Adams PD. Iterative model building, structure refinement and density modification with the *PHENIX AutoBuild* wizard. Acta Crystallogr. D Biol. Crystallogr. 2008; 64(Pt. 1):61–69. [PubMed: 18094468]
70. Spurrier B, Sampson JM, Totrov M, Li H, O'Neal T, Williams C, Robinson J, Gorny MK, Zolla-Pazner S, Kong XP. Structural analysis of human and macaque mAbs 2909 and 2.5B: Implications for the configuration of the quaternary neutralizing epitope of HIV-1 gp120. Structure. 2011; 19:691–699. [PubMed: 21565703]
71. Appleton BA, Wu P, Maloney J, Yin J, Liang W-C, Stawicki S, Mortara K, Bowman KK, Elliott JM, Desmarais W, Bazan JF, Bagri A, Tessier-Lavigne M, Koch AW, Wu Y, Watts RJ, Wiesmann C. Structural studies of neuropilin/antibody complexes provide insights into semaphorin and VEGF binding. EMBO J. 2007; 26:4902–4912. [PubMed: 17989695]
72. Emsley P, Lohkamp B, Scott WG, Cowtan K. Features and development of Coot. Acta Crystallogr. D Biol. Crystallogr. 2010; 66(Pt. 4):486–501. [PubMed: 20383002]
73. Adams PD, Afonine PV, Bunkóczi G, Chen VB, Davis IW, Echols N, Headd JJ, Hung L-W, Kapral GJ, Grosse-Kunstleve RW, McCoy AJ, Moriarty NW, Oeffner R, Read RJ, Richardson DC, Richardson JS, Terwilliger TC, Zwart PH. PHENIX: A comprehensive Python-based system for macromolecular structure solution. Acta Crystallogr. D Biol. Crystallogr. 2010; 66(Pt. 2):213–221. [PubMed: 20124702]
74. Lovell SC, Davis IW, Arendall WB III, de Bakker PIW, Word JM, Prisant MG, Richardson JS, Richardson DC. Structure validation by Cα geometry: φ,Ψ and Cβ deviation. Proteins. 2003; 50:437–450. [PubMed: 12557186]

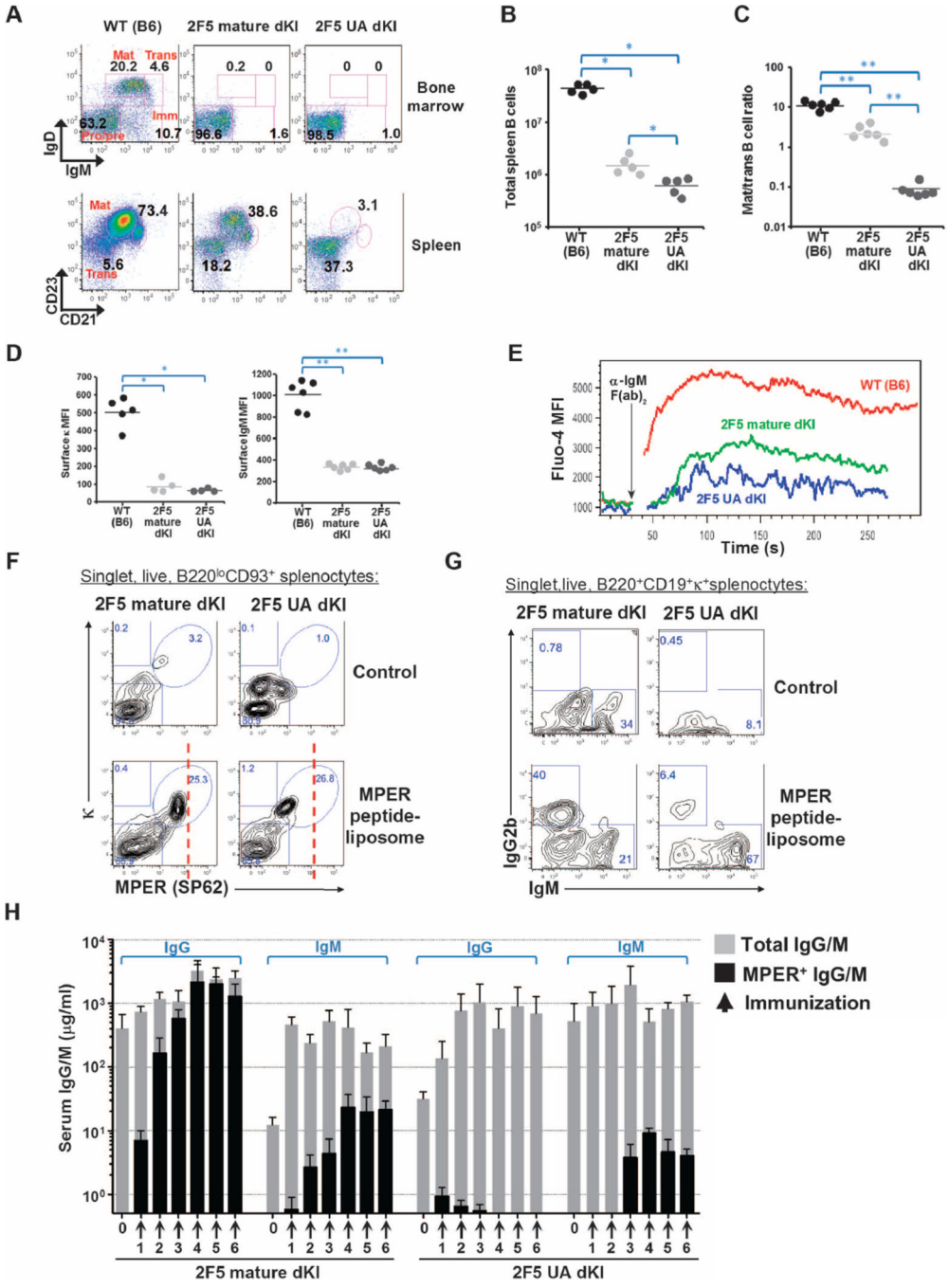

Fig. 1. Immune tolerance in 2F5 mature and UA dKI mice

(**A** to **D**) B cell development in 2F5 mature and UA dKI mice, compared to wild-type (WT) (B6). (A) Percentages in progenitor/precursor (pro/pre), immature (imm), transitional (trans), and mature (mat) subsets. (B) Total numbers of B cells in spleen. (C) Ratios of mature to transitional splenic B cells. (D) BCR densities on newly formed/transitional ($CD21^{-}CD23^{-}$) splenic B cells, measured by median fluorescence intensity (MFI) of κLC or IgM expression [see table S8 for summary of statistical test results for (B) to (D)]. (**E**) Ex vivo proximal signaling responses to BCR crosslinking in transitional splenic B cells from

naïve 2F5 mature or UA dKI and control B6 mice based on Ca^{2+} levels (Fluo-4 MFI) before/after anti-IgM stimulation. (**F**) Expansion of MPER-reactive splenic transitional B cells in 2F5 mature and UA dKI mice immunized six times with MPER peptide-liposomes. Control, saline-injected mice; SP62, MPER peptide QQEKNEQELLELDKWASLWN-biotin. (**G**) Comparison of IgG-switched splenic B cells in immunized 2F5 mature and UA dKI mice. (**H**) Total and MPER-specific serum IgG/IgM levels in immunized 2F5 mature and UA dKI mice, compared to B6. X axis arrows, number of MPER peptide-liposome injections after which serum was collected; 0, prebleed in naïve mice. Error bars represent means ± SEM [see figs. S7 and S8 for replicate images for (A) and (E), respectively].

A

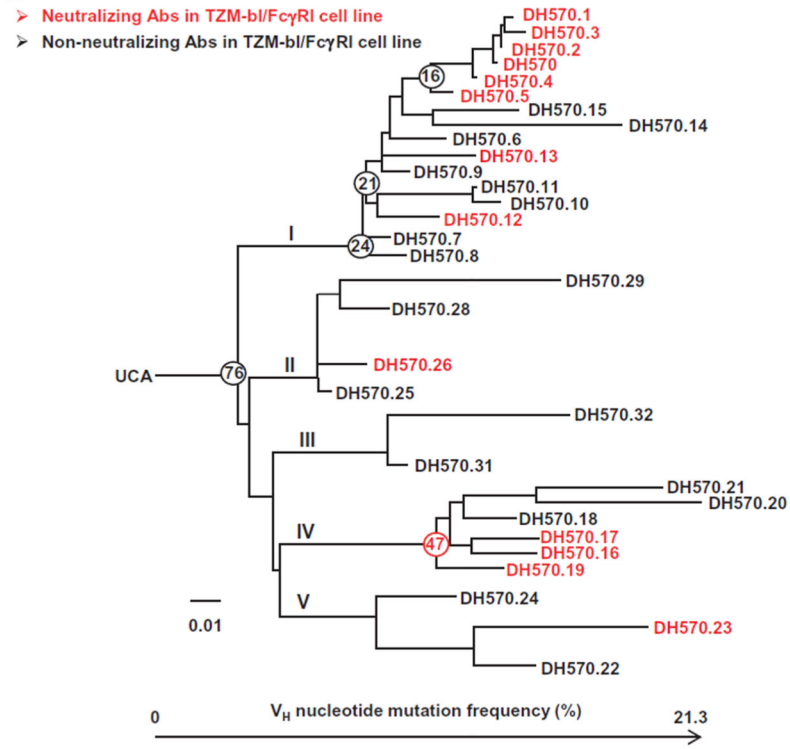

B

Ab	V_H	D_H	J_H	V_H mutation (%)	HCDR3	Isotype	V_K	J_K	V_K mutation (%)	LCDR3
DH570	4–B	5–6	5	12.2	21	G1	1–23	1	11.1	7

C

	Neutralization IC_{50} (μg/ml)											
	W61D (TCLA)		HXB2		SC422661.8		JR-FL		WITO4160.33		MuLV	
	Tier 1A		Tier 1B		Tier 2		Tier 2		Tier 2		Neg control	
Ab_name	TZM-Bl	TZM-Bl/FcγRI	TZM-Bl	TZM-Bl/FcγRI	TZM-Bl	TZM-Bl/FcγRI	TZM-Bl	TZM-Bl/FcγRI	TZM-Bl	TZM-Bl/FcγRI	TZM-Bl	TZM-Bl/FcγRI
DH570.UCA1	>50*	>50*	>50*	>50*	>50*	>50*	>50*	>50*	>50*	>50*	>50*	>50*
DH570.UCA2	>50*	>50*	>50*	>50*	>50*	>50*	>50*	>50*	>50*	>50*	>50*	>50*
DH570.IA76	>50*	>50*	>50*	>50*	>50*	>50*	>50*	>50*	>50*	>50*	>50*	>50*
DH570.IA47	>50	4.09	>50	0.06	>50	0.94	>50*	1.20*	>50	25.92	>50*	>50*
DH570.IA24	>50	>50	>50	>50	>50	>50	>50	>50	>50	>50	>50	>50
DH570.IA21	>50	>50	>50	>50	>50	>50	>50*	>50*	>50	>50	>50*	>50*
DH570.IA16	>50	>50	>50	>50	>50	>50	>50*	>50*	>50	>50	>50*	>50*
DH570	>50	14.87	>50	25.28	>50	15.60	>50	>50	>50	26.46	>50	>50
DH570.4	>50	3.05	>50	0.22	>50	>50	>50	>50	>50	31.25	>50	>50
DH570.9	>50	>50	>50	>50	>50	>50	>50	>50	>50	>50	>50	>50

Fig. 2. DH570 clonal lineage members neutralize tier 1 and 2 HIV isolates in TZM-bl/FcγRI assay

(**A**) Phylogenetic relationship of 32 mAbs in DH570 clonal lineage. The mAbs neutralizing tier 1 and/or tier 2 HIV isolates in TZM-bl/FcγRI assay are highlighted in red. The mutation frequency of the most mutated antibody is 21.3% (DH570.20). (**B**) Immunogenetics of DH570 mAb. (**C**) Neutralization activity of representative observed and inferred IAs in the DH570 clonal lineage. Neutralization assays were performed in both TZM-bl and TZM-bl/

FcγRI cell lines. IC_{50}s reported as median values of at least two independent experiments except where noted by asterisks.

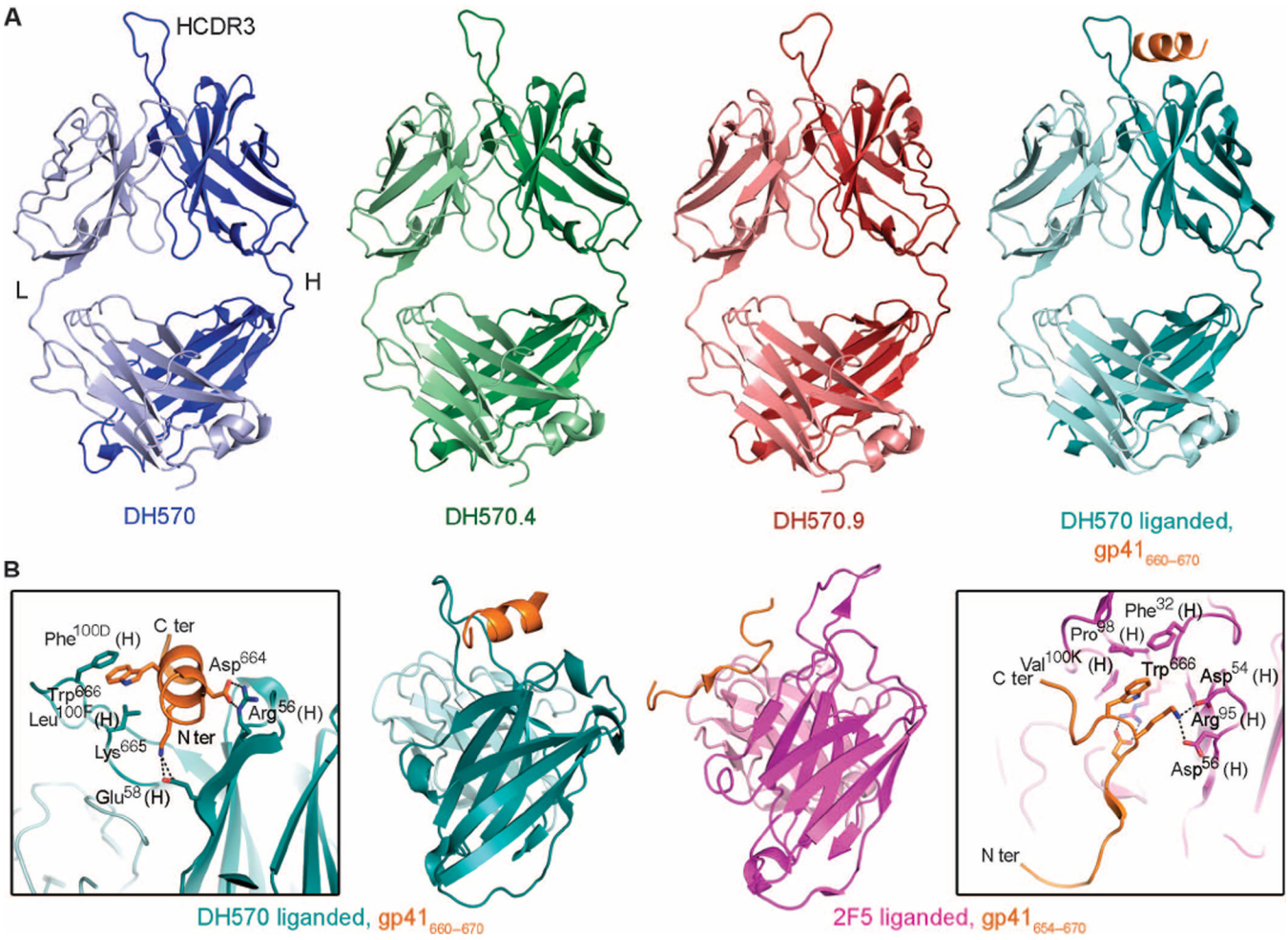

Fig. 3. Crystal structures of DH570 clonal lineage antibodies

(**A**) Structure of unliganded DH570 (blue), DH570.4 (green), DH570.9 (red), and DH570 (cyan) in complex with $gp41_{660–670}$ peptide (orange). (**B**) Superposition of liganded DH570 (cyan) and liganded 2F5 (magenta) (28) with insets respectively highlighting the different peptide antigen conformations (orange) as well as the different antibody-antigen contacts between the two complexes. C ter, C terminus; N ter, N terminus.

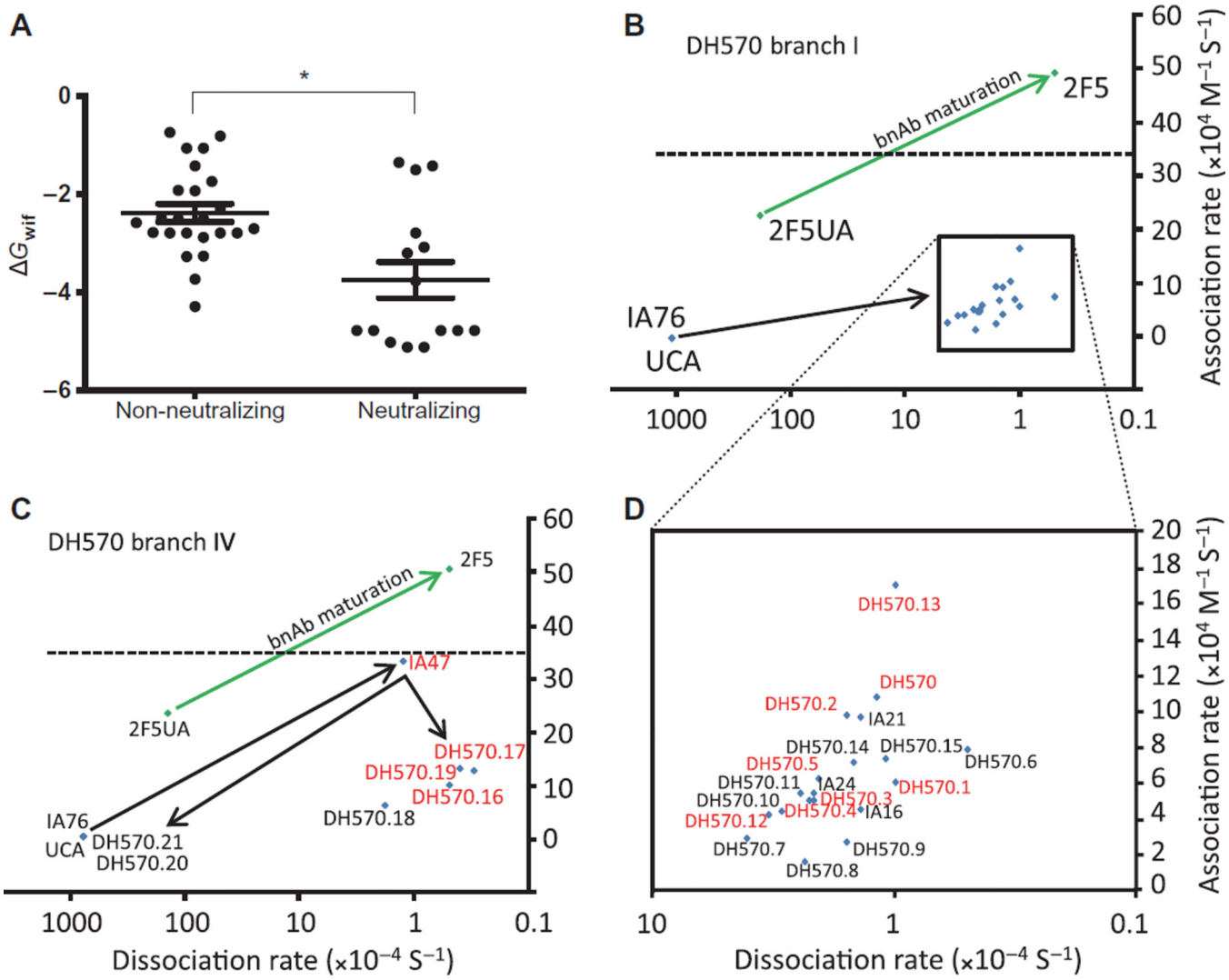

Fig. 4. DH570 members exhibit slower association rates relative to 2F5

(**A**) Computed lipid insertion propensity scores ΔG_{wif} (kcal/mol) of HCDR3 and LCDR3 (summed) are more favorable for neutralizing than nonneutralizing DH570 clonal members (*P = 0.0054, Wilcoxon-Mann-Whitney test with Benjamini-Hochberg correction; n = 23 and 15; lines denote means ± SEM). (**B** to **D**) Association rate (K_a, on-rate) and dissociation rate (K_d, off-rate) constants of DH570 clonal lineage branch I (B) and IV (C) antibodies binding to MPER peptide-liposome with greater detail of branch I antibodies shown in (D). Dashed lines represent association rate ceiling. Arrows show maturation pathways derived from phylogenetic tree of the DH570 clonal lineage in Fig. 2A. Data in (B) to (D) were obtained by BLI and were representative of two independent association and dissociation analyses. Kinetic rates data plotted here are listed in table S6 and each BLI curve is plotted in fig. S6.

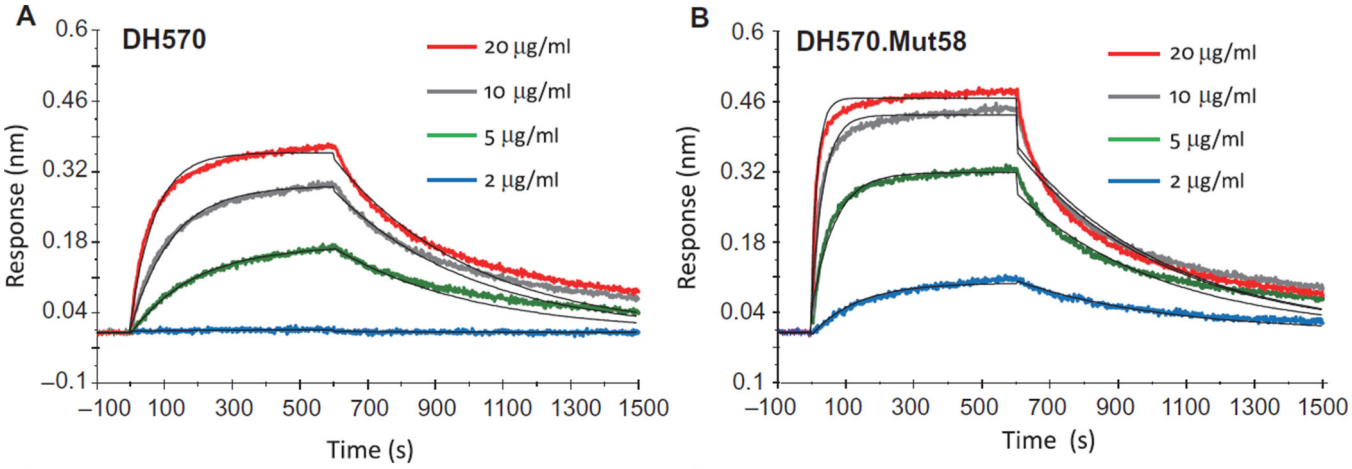

C

Binding kinetics

Ab ID	K_a ($\times 10^4$ M^{-1} s^{-1})	K_d ($\times 10^{-4}$ s^{-1})	K_d (nM)
DH570	2.87	24.1	83.7
DH570.Mut58	12.9	23.3	17.8

D

Neutralization of W61D in TZM-bl cells

Ab ID	# Assays	Median IC_{50} (µg/ml)	Range IC_{50} (µg/ml)
DH570	9	>50	All >50
DH570.Mut58	7	32.5	(11.2–46.1)

Fig. 5. DH570 mutant acquires high affinity binding and neutralization capacity in the TZM-bl neutralization assay

(**A** and **B**) BLI sensorgrams of MPER peptide-liposome binding by DH570 Fab (A) and DH570.Mut58 Fab (B) at different antibody concentrations (2, 5, 10, and 20 µg/ml). (**C**) Measured kinetic rates (K_a and K_d) and dissociation (K_d) constants of DH570 and DH570.Mut58 binding to MPER peptide-liposomes. (**D**) Neutralization activity of whole IgG1 DH570 and DH570.Mut58 against W61D in the TZM-bl assay. BLI measurements in (A) to (C) are representative of two independent experiments (see fig. S9 for replicate plot and kinetic data).